LA-3655

C.3

# LOS ALAMOS SCIENTIFIC LABORATORY
## of the
## University of California
### LOS ALAMOS • NEW MEXICO

Fuel Cycle Cost Implications of

Liquid Plutonium Reactor Fuel

This report expresses the opinions of the author or authors and does not necessarily reflect the opinions or views of the Los Alamos Scientific Laboratory.

# LOS ALAMOS SCIENTIFIC LABORATORY
## of the
## University of California
### LOS ALAMOS • NEW MEXICO

# Fuel Cycle Cost Implications of

# Liquid Plutonium Reactor Fuel

**Work done by:**

C. A. Anderson, K-3
M. E. Battat, K-1
D. J. Dudziak, K-1
D. N. Dunning, K-2
W. H. Hannum, K-1
R. J. LaBauve, K-1
W. J. Maraman, CMB-11
R. H. Perkins, K-2
J. J. Prabulos, Jr., K-1
G. L. Ragan, K-1

**Report compiled by:**

W. H. Hannum, K-1

TABLE OF CONTENTS

# LIST OF TABLES

# LIST OF FIGURES

## ABSTRACT

Probable fuel cycle costs for a liquid plutonium alloy fuel have been studied for a particular fast breeder reactor application. The fuel cycle costs for the liquid fuel are at least as attractive as those derived for the solid-fuel reference case, and additional studies have indicated areas in which the liquid fuel would have a definite fuel cycle cost advantage over solid fuels.

## ACKNOWLEDGMENTS

# 1. INTRODUCTION AND SUMMARY

The initial interest in the use of a liquid plutonium alloy reactor fuel, as in other liquid fuels, arises from the potential for simplified handling.[1] Current work on this concept, however, has concentrated on the use of this fuel in a sealed capsule.[2] Even in this conventional form, the fuel retains several distinct advantages associated with the liquid state. That is, fuel swelling cannot lead to mechanical straining of the container, phase changes will not occur in any realistic operating situation, and thermal bonding and good heat transport are inherent.

Metallic alloy fuels have further potential advantages. The hard neutron spectrum associated with a metallic fuel gives a high neutron multiplication ($\eta \simeq 2.7$), thus suggesting the possibility of a very high-gain breeder (BR > 1.6).[3] Of equal or greater significance is the large expansion coefficient associated with a liquid metal. With the present container material (a tantalum-tungsten alloy), which has a low expansion coefficient, the entire liquid volumetric expansion is effective in reducing the core-average fuel density. Thus, a large, negative, prompt temperature coefficient of reactivity is assured.

With this list of desirable attributes -- high breeding gain, large favorable power reactivity coefficient, and fuel element lifetime not limited by mechanical fuel damage -- it is of interest to ask how this fuel system can be used in a practical reactor concept. Most previous work relative to applications of liquid plutonium fuels has considered doubling time to be a suitable measure of the performance potential of the system.[3] For the near-term, fuel cycle costs are perhaps more

significant than doubling time. As an illustration of the economic potential of liquid plutonium in the near-term, we consider here the direct substitution of liquid plutonium fuel elements into the system described in Ref. 4. This solid-fuel case does not reflect recently proposed modifications and updating.[5] A brief description of this case is given in Section 1.1.

Certain aspects of this particular design are inappropriate for use with the present liquid-fuel concept. Those which could easily be handled, such as the extraneous (for our case) graphite separator, were adjusted. Other features, such as outer core radius and the use of an oxide blanket, were retained. In spite of the many accommodations necessary to adjust to the restraints imposed by this adverse design basis, fuel cycle costs similar to those for a solid fuel were obtained for a liquid-fuel case, with no major extrapolation except in the assumed burnup capability. All the other desirable attributes associated with the liquid-plutonium systems (such as safety and stability) are retained. Table 1.1 summarizes the fuel cycle cost comparison between the reference solid-fuel case and the case in which the solid-fuel elements are replaced by liquid-fuel elements.

Certain performance attributes of such a liquid-fuel system have been investigated, as an aid in understanding the system requirements and capabilities. The resulting fuel cycle appears to be reasonable for utility use and contains some flexibility. In addition, fuel residence time appears to be long enough in this application to warrant serious consideration of partial refuelings, at least for the blanket. Reactivity control requirements do not appear prohibitive, but, again, a partial refueling would be desirable. In-core instrumentation is likely to be required as for any large fast system.

For any modular system, power distributions are distinctly nonuniform, and power shifts from core to blanket would be significant in a single-batch loading scheme. The power shifts are likely to require a

6

TABLE 1.1

Summary Comparison of Characteristics

| | Solid-Fuel Case[a] | Liquid-Fuel Substitution[b] | Liquid-Fuel Modest Extrapolation[c] |
|---|---|---|---|
| Fuel Cycle Cost [mil/kWhe] | | | |
| Fabrication | 0.21 | 0.32 | 0.11 |
| Capital & Shipping | 0.02 | 0.01 | nil |
| Reprocessing | 0.12 | 0.09 | 0.04 |
| Inventory | 0.68 | 0.45 | 0.41 |
| Blanket | 0.24 | 0.41 | 0.41 |
| Net Pu credit | (0.38) | (0.25) | (0.39) |
| Net Total | 0.89 | 1.03 | 0.58 |
| | | | |
| Other Factors | | | |
| Total power [MWt] | 2500 | 2500 | 2500 |
| Core power [MWt] | 2100 | 1900 | 1650 |
| Breeding ratio | 1.49 | 1.37 | 1.65 |
| Loading [kg fissile Pu] | 3700 | 2700 | 2350 |

[a]See Ref. 4.

[b]See Section 3.

[c]See Section 5.

modest derating of the core. The local power peaks associated with the liquid-fuel case do not add a substantial burden to thermal performance beyond that normally associated with modular systems.

Internal fuel circulation has been considered, and no unique difficulties have been found.

Several demonstrated methods for reprocessing spent liquid metal alloy fuel have the potential for appreciable cost saving, but require further development. The effect of the reprocessing method on the composition of the in-core fuel also requires further consideration.

Modest extrapolation from the present case in such areas as the use of thin-wall or reduced cross-section containment and the use of a metal blanket show a potential for improving fuel cycle costs. Should any of these developments be shown to be feasible, a fuel cycle cost advantage for the liquid-fuel system would be obtained. Parameters for this case are summarized in Table 1.1.

Much work remains in defining an optimum system to utilize the presently demonstrated capability. Certain data, such as a burnup limit, need to be established.


## 2. SELECTION OF REFERENCE SYSTEM PARAMETERS

### 2.1 Ground Rules

Optimization of a system includes detailed analyses of a wide variety of factors and, in general, must progress through several stages. The present study is intended as an illustration of potential and not as an optimization. Thus, it is reasonable to make a number of arbitrary specifications without reference to optimization. The results of this study can then be used to isolate areas in which substantial progress can be made toward obtaining an optimum.

Two major features of the present study are: (1) The system selected uses a liquid-plutonium fuel element design for which a great deal of experience is available. All extrapolations from demonstrated performance are clearly identifiable, and there are no known factors which preclude the performance indicated. (2) Maximum use is made of published results for system components other than the core fuel element.

The first condition was selected to give a conservative estimate of the potential of this fuel system and to allow a clear indication of the incentive for further development. The reference fuel element is thus restricted to a sealed tantalum (or tantalum alloy) capsule of about 1-cm diameter and a nominal wall thickness of 0.05 cm. Sodium coolant is used.

The second condition is imposed for two reasons: to reduce the amount of work required to obtain an indication of fuel cycle costs, and, more significantly, to make the results obtained comparable with those of other studies.

At the time this study was initiated, six major studies of 1000-MWe plants were available.[4,6-12] All of these used refractory blanket fuels. The reference case in this paper arbitrarily assumes an oxide-fueled blanket. With an oxide-fueled blanket, it is necessary to speak of a totally external breeder,[2] since the moderator (oxide) must be separated from the tantalum used to contain the plutonium in present liquid-fuel concepts. From the various arrangements of totally external breeders which have high power capability, the modular arrangement was chosen. While there are certain advantages to this choice,[11] this, in fact, represents an arbitrary selection. A less-moderating blanket permits both greater design flexibility and substantially improved performance. Section 5 includes a discussion of the potential of the system with a less-moderating blanket.

Since the published 1000-MWe studies included modular cases with oxide blankets, one of them was used as a basis. The study used was that by Westinghouse,[4] but a similar adaptation of the Atomics

International study,[9] or, for that matter, of any of the systems except the Combustion Engineering study,[7] which is not well suited to external breeding, could have been made.

The reference solid-fuel case is a seven-module design. Each module is tall (length 190 cm; diameter ≈72 cm) and weakly coupled to adjacent modules through thick radial blankets. The tall modules are used primarily to enhance the negative components of the sodium void effect. The core fuel elements are sodium-bonded carbide, clad in a 300-series stainless steel. The fuel pellet diameter is 0.68 cm, and the clad is 0.025 cm thick by 0.76 cm diameter. Fission-product venting to the primary coolant is assumed. There is no pretense that this is a fully developed and tested fuel element; however, the design is not unrealistic.

The blanket design in the reference solid-fuel case is more conventional. A 1.07-cm diameter oxide fuel pellet in an 0.05-cm-thick can is used. The core fuel element pitch is relatively loose (high sodium fraction); the blanket uses a relatively tight pitch. The modules are further separated, both neutronically and mechanically, by rows of graphite rods.

## 2.2 Calculational Model

Survey calculations are readily done for a modular geometry, but detailed design calculations involve some difficult representational problems. For survey work, the characteristics of modular arrangement can be considered to be between those of a single module and those of an infinite array of identical modules. Calculationally, these limiting cases are described as being single cells with a zero return flux and with a zero flux gradient at the boundary, respectively. Because of the small number of space points and the generally tight neutronic coupling within a single cell, this pair of calculations can normally be done in less time than can the calculation for a uniform system. For the case selected, the individual modules are tall, so that the axial

leakage can be approximately accounted for by a buckling term. The interpolation between free and reflected modules can be estimated from a surface area ratio between reflected and free boundaries.

The calculational model used for all the studies reported herein is shown in Fig. 1. All cases were calculated with both free and reflected boundaries. Some reactor parameters, such as breeding factors (see Appendix A), are inferred from single module calculations, in conjunction with a knowledge of module and reactor peripheries. All calculations, except as noted, have been done in $S_4$ approximations (DTF[13] and DDF[14] codes) with Hansen-Roach 16-group shielded cross sections.[15]

## 2.3 Major Parameters and General Range of Interest

The major components of reactor fuel cycle cost are fabrication and recycle costs, inventory charges, and net plutonium costs. In each of these areas, a liquid alloy fuel has a potential cost advantage over a solid fuel. There are also factors which tend to compromise each of these advantages. The purpose of this study is to identify a range of conditions for which the liquid fuel may have a net fuel cycle advantage. The detailed analysis of actual costs is given in Section 3.

### 2.3.1 Capsule Size

To obtain a low fabrication cost contribution to the fuel cycle cost, it is necessary to extract a large amount of energy per unit fabrication cost. This means, of course, a combination of low unit cost and high burnup. Since tantalum tubing, the presently envisioned container material, is moderately expensive, the energy output per fabrication cycle must be kept relatively large. To a first-order approximation, fabrication cost per fuel element is independent of dimensions.[16] Thus, large capsules are likely to have an economic advantage, in that more energy is available per unit fabrication cost.

CORE

RADIAL BLANKET

REFLECTOR

$\phi = 0$ OR REFLECTED

$H$

$O$

$R$

$R_1$  $R_2$  $R_3$

¢
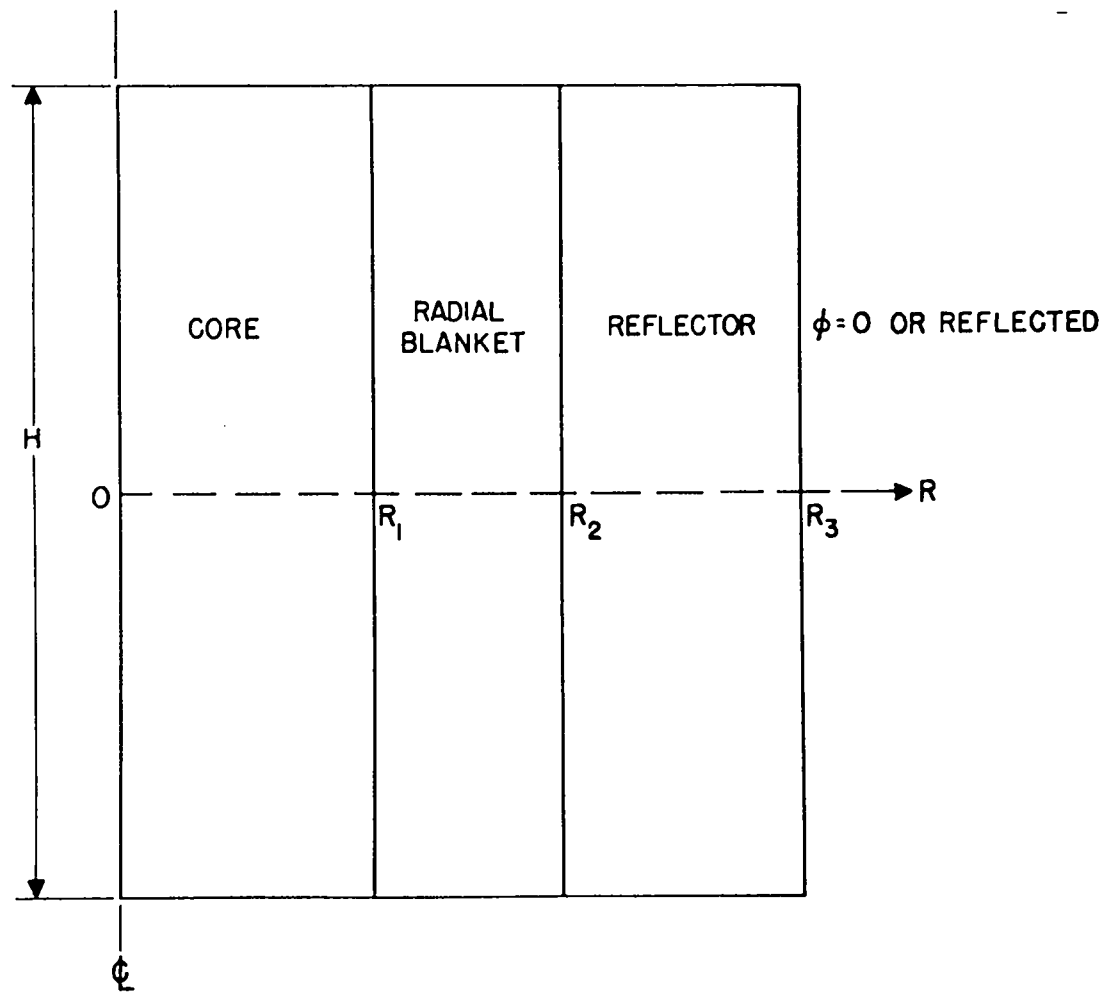
Fig. 1.  Calculational Representation

## 2.3.2 Burnup Limits

In a fast reactor, there will generally be a fuel cycle cost advantage to obtaining the highest feasible burnup of the fuel. For a given capsule, the contribution of the fabrication cost to the fuel cycle cost is inversely proportional to the burnup. Since data on the properties of liquid fuels after high burnup are not presently available, it is impossible to predict accurately the burnup capability of the fuel.[17] However, since this is a major factor in evaluating fuel cycle costs, it is necessary to select a reference criterion against which both performance and potential can be evaluated. For solid fuels, a reference criterion of an average 100,000 MWd/T (100 MWd/kg) is frequently used.[11] The limiting factor assumed for solid fuels is gross swelling of the fuel, leading to straining of the container. This straining does not occur for liquid fuel. Thus, there is no reason to expect the 100 MWd/kg criterion to be appropriate for liquid fuels. A potential inherent limit on burnup capability of the liquid fuel is the gross accumulation of soluble fission products.[18] While no limiting mechanism is specifically proposed, it is assumed for this study that such a limiting concentration of soluble fission products does exist. In order to assign a numerical value to this limiting value, it is further assumed that this concentration is obtained when the integrated number of fissions per unit volume is approximately equal to that of a mixed oxide fuel after 100 MWd/kg ($\simeq 1$ gf/cc).* Again, it is emphasized that this criterion, like that of 100 MWd/kg, is justified neither by experimental data nor by theoretical or analytic projection. It is meant only as a criterion against which performance and potential can be measured. (The UK PFR concept, for example, is based on an anticipated 60 MWd/kg burnup.[19])

---

* See Appendix B.

13

It may be more realistic to consider reactivity loss as limiting the burnup capability of a liquid fuel. In the present study, it is assumed that sufficient control swing is available to accommodate the implied reactivity swing. This is not necessarily an optimum solution. Some comments are given in Section 4.1 on the control required for the liquid fuel and for the solid fuel.

### 2.3.3 Heat Transfer Limits

Heat transfer limits enter the calculation of fuel cycle costs by way of the inventory charge. The inventory charge can be considered in two parts: that for in-core inventory and that for out-of-core. The in-core charge is inversely proportional to the specific power (or, more explicitly, to the power per unit value of fuel). The specific power attainable may be considered in terms of a single fuel element: How much power can be removed from it, and how much fuel does it contain? This assumes that the coolant itself does not limit the thermal performance of the element. Three items are normally considered to be potentially limiting: fuel temperature, container temperature, and container stress. For a liquid fuel, disengagement of volatile fission products and internal fuel circulation from natural convection must also be considered (see Section 4.3). Fuel temperature, for the liquid fuel, is not a significant limit, because the boiling point of the liquid metal alloy is about 3000°C. Thus, no phase change of the fuel is expected even under accident conditions. For a solid fuel, fuel melting is a pertinent design consideration, particularly since fuel slump and consequent reactivity insertion can be expected in the case of accidental gross fuel melting. For a solid fuel, it is thus necessary to use small diameter pins[4-12] (about 0.5 cm o.d.) to limit the anticipated fuel centerline temperature. Other considerations unique to solid fuel elements reinforce this requirement: e.g., plutonium migration, void migration, and swelling rates.[11] For a liquid fuel, fuel temperature limits do not preclude the use of large capsule diameters.

14

Container thermal stress and temperature rise are both proportional to the heat flux through the wall. In addition, the thermal stress is proportional to wall thickness and the coefficient of thermal expansion. For design concepts in which it is assumed that stainless steel is a suitable container material, the trend is toward a thin ($\approx$0.02 cm) container wall. Even at this, the heat flux is limited to $\approx$400 W/cm$^2$. For Ta-5 w/o W (Ta-5W) capsules ($\approx$0.05-cm-wall), a heat flux of several times this amount is permissible. In the cases considered here, thermal stressing of the capsule wall (even with 0.05-cm-wall) is not a limiting factor.

For a liquid fuel, this leaves only container temperature as the limiting factor for heat transfer. The container itself is a refractory metal (Ta-5W). However, the intergranular penetration of plutonium into tantalum alloys is temperature dependent. The criteria selected for a Pu-Co-Ce fuel in carburized capsules are maximum interface temperatures of 750°C in an average channel and of 800°C at the hottest point. These temperatures are considered to be conservative (see Ref. 17). The maximum fuel-container interface temperature is determined by a combination of factors: coolant inlet temperature, coolant temperature rise, and wall and film drops. The minimum inlet temperature (460°C) for the Pu-Co-Ce fuel is set by the melting point of the fuel ($\approx$435°C). The minimum coolant temperature rise is normally set by coolant velocity or pressure drop constraints. The maximum wall and film drops are thus determined and limit the allowable heat flux. At a given heat flux, the specific power is proportional to the heat transfer area per unit mass of fuel. This suggests small-diameter fuel pins and low-density fuel for high specific power and low in-core inventory charge.

On the other hand, the fabrication cost considerations of Section 2.3.1 and breeding considerations to be discussed in Section 2.3.5 both argue for large capsule diameter and high-density fuel. An appropriate compromise is obviously required to minimize overall fuel cycle costs.

In reaching this compromise, a significant flexibility is available with a modular system. In any reactor, criticality requirements must be respected. With an array of cores, however, criticality requirements can be met by varying the number of modules and their configuration. For this survey, the size and number of fuel capsules are selected prior to specifying the fissile content of the fuel. Criticality restraints can then be met either by choosing a fuel and dividing the fixed number of capsules into modules and letting the number of modules vary as required, or, alternatively, by assembling the given number of capsules into a specified array and varying the fuel composition for criticality. (This latter process is analogous to varying enrichment.)

### 2.3.4  Out-of-Core Factors

The out-of-core inventory cost depends on turnaround (cooling, reprocessing, and fabrication) time, since this determines the value of fuel in the out-of-core circuit. The practical times required for turnaround operations have not been well defined for fuels of current commercial interest. However, in a relative sense, there is a potentially great advantage for metal fuels (solid or liquid) if a pyrochemical method is used.[20]

As is discussed in Section 3.2, if a volumetric limitation on fuel burnup capability (e.g., 1 gf/cc) is used, then for a fixed fuel volume, a reduction in fuel density will reduce the out-of-core inventory. Thus, inventory charges, both in-core and out-of-core, would be decreased by low-density fuel. On the other hand, if a fractional burnup limit is controlling (e.g., 10% BU), then to a first-order approximation, the out-of-core inventory charge depends primarily on the actual turnaround time.

16

### 2.3.5 Fuel

The remaining major fuel cycle cost component is the net plutonium charge or credit. This is approximately proportional to the breeding gain. As has been discussed in Ref. 2, there is a distinct breeding advantage in the use of a high-plutonium-density fuel, to avoid excessive neutron loss to parasites. Since the preceding factors have largely favored low-plutonium-density fuels, a compromise not unlike that to optimize doubling time (see Ref. 2) is indicated. Thus, a fuel parameter range selected for favorable doubling time may be considered a reasonable starting point for fuel cycle cost optimization.

### 2.4 Selection of Specific Case

#### 2.4.1 Number of Capsules

Based on the above considerations, the first case investigated used a large capsule diameter. An outside diameter of 1.5 cm (0.6 in.) was selected as an upper limit (a 40% extrapolation in diameter from LAMPRE I experience).[21] A Ta-5W capsule wall of 0.05 cm (0.020 in.), as has been used in extensive out-of-core testing,[17] is specified.

The remaining parameters (exclusive of the fuel) are pitch (center-to-center fuel pin spacing) and number of capsules. The factors that can be considered to be limiting are the coolant velocity and pressure drop (which argue for a large pitch), fuel-capsule interface temperature (which argues for a high flow* and many capsules), and neutronic considerations (which argue for low sodium content to avoid spectrum degradation and few capsules to help reduce the tantalum-plutonium ratio). An optimization study is beyond the scope of this report, but certain generalizations have been used to indicate a likely case of interest. The analytic formulation and the material constants used to describe the relevant case are given in Appendix C. Figure 2 is a plot of the

---

* The high power capability of the capsules and the large core height (190 cm) of the reference case suggest that a large coolant flow channel will be required to avoid an excessive temperature rise in the coolant.
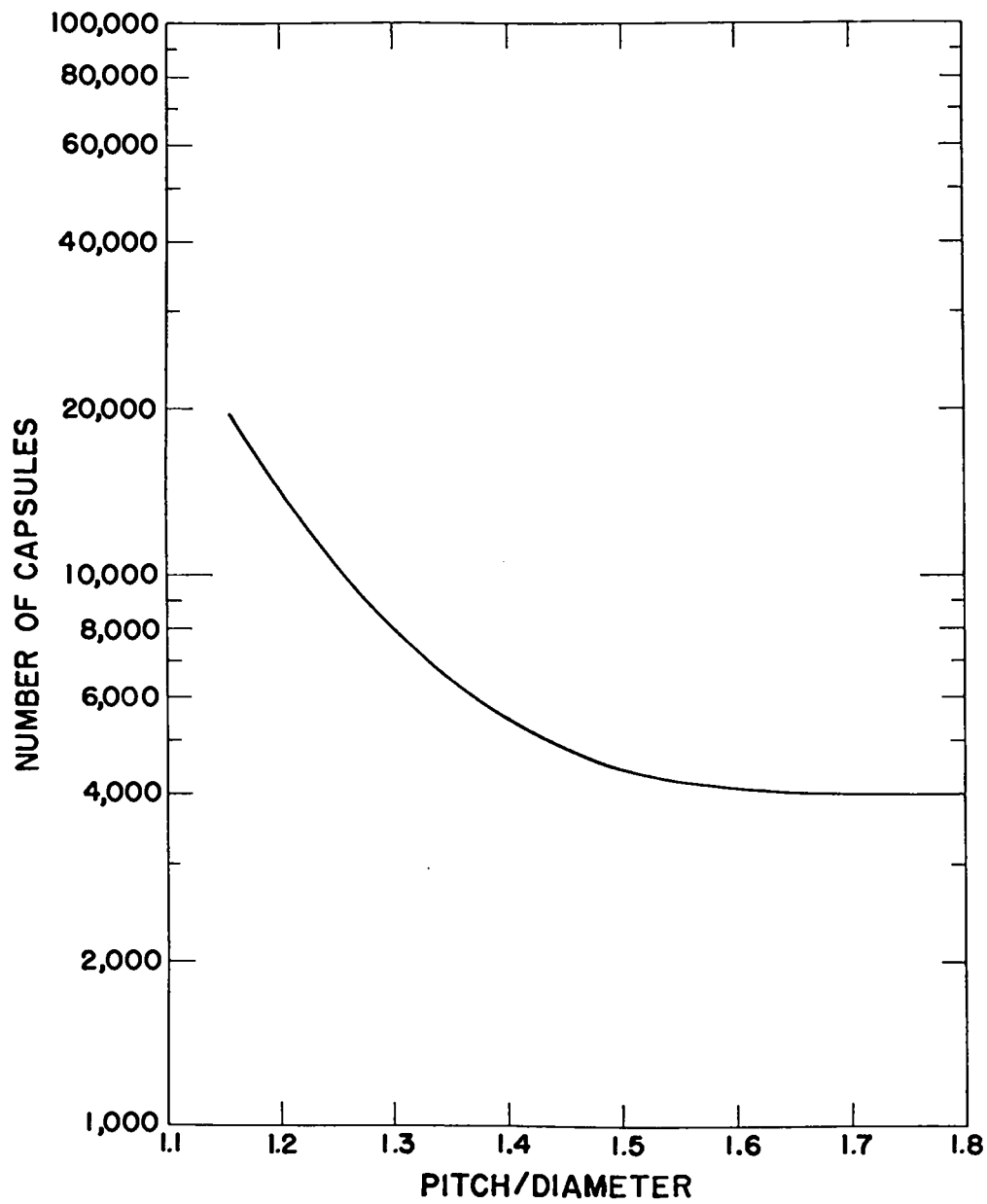
Fig. 2. Estimated Minimum Number of Capsules Required to Satisfy
Temperature, Pressure Drop, and Velocity Limits

estimated minimum number of capsules required to satisfy temperature, pressure drop, and velocity limits versus pitch-to-diameter (P/D) ratio. (This is a plot of the locus of the minima of the curves shown in Fig. 6.) Thermal stress limits (see Appendix D), which require at least 530 sealed capsules or 370 vented capsules with a 1.5-cm diameter, are less stringent than those limits shown in Fig. 2.

The advantage to a low P/D ratio is that it favors neutron economy by virtue of reduced moderation. However, for a low P/D ratio, the pressure drop consistent with suitable interface temperatures increases rapidly, requiring a rapid increase in the number of elements. Since this represents an increase in the tantalum content of the core, it does not seem advisable to go far in that direction. Thus, for the set of ground rules and initial parameters used here, a P/D ratio of 1.5 is selected as a reasonable value. It further appears from this that about 4500 fuel elements should be adequate for about 1900 MWt in this arrangement.

Thermal calculations performed for the range selected indicate that the Nusselt number used in Appendix C is unduly conservative. Thus, further reduction in number of capsules by ≈20% is possible. It is convenient to specify a number of capsules which can be neatly assembled into seven modules. The number of capsules selected is 7 · 19 · 27 = 3591. The fuel element parameters and restrictions selected for this study are summarized in Table 2.1. With the values selected, there should be no outstanding problem in using equipment as in Ref. 4. The performance values included in Table 2.1 are based on confirmatory HTHX[22] calculations. It may be noted that this set of parameters does not depend on the fuel density used.

### 2.4.2 Fuel Properties

It is assumed in the present study that any fuel between 3 and 8 g Pu/cc can be used and that the fuel lifetime is limited by gross accumulation of fission products to 1.0 gf/cc (see Appendix B). This

TABLE 2.1

Parameters for Reference Liquid-Plutonium Fuel Case

Specified Parameters

| | | |
|---|---|---|
| Core power | [MWt] | 1900 |
| Capsule diameter | [cm] | 1.5 |
| Capsule wall thickness | [cm] | 0.05 |
| P/D | | 1.5 |
| Fuel length | [cm] | 190 |
| Coolant inlet temperature | [°C] | 460 |
| Core sodium flow capability | [kg/sec] | $8.2 \times 10^3$ |
| Number of capsules | | 3591 |

Calculated Parameters

| | | |
|---|---|---|
| Coolant outlet temperature | [°C] | 644 |
| Maximum fuel-capsule interface temperature | [°C] | 744 |
| Core coolant pressure drop | [psi] | 10.3 |
| Thermal stress | [$10^3$ psi] | 8.3 |
| Fuel volume | [liter] | $1.05 \times 10^3$ |

corresponds to 20% plutonium burnup for 5 g Pu/cc fuel. No fertile material other than $^{240}$Pu is present in the fuel. Since the isotopic plutonium mix does not change greatly through life, a given net fissile loss of plutonium in the core corresponds to a similar fractional total loss, all of which must be by fission (except for the small $^{242}$Pu build-up). Thus, a given burnup corresponds to a similar net loss in fissile material.

For fuels in the range considered, some properties are given in Table 2.2 (see also Appendix F). Mid-life fuel (0.5 gf/cc) is used in all nuclear calculations.

A series of neutronic calculations was run for Pu-Co-Ce cores containing, at beginning-of-life, 4.1, 5.0, or 6.1 g Pu/cc fuel and the blanket described in Ref. 4. The core configuration and composition for this series are given in Table 2.3; volume fractions quoted were computed

TABLE 2.2

Fuel Properties

| Beginning-of-Life Pu Content (g Pu/cc) | Mid-Life Pu Density (g Pu/cc) | Initial Loading | | |
|---|---|---|---|---|
| | | ρ (g/cc) | w/o Co | w/o Ce |
| 3.0 | 2.5 | 8.81 | 10.6 | 55.1 |
| 4.0 | 3.5 | 9.32 | 10.0 | 47.1 |
| 5.0 | 4.5 | 9.93 | 9.6 | 39.9 |
| 6.2 | 5.7 | 10.65 | 9.1 | 33.0 |
| 7.2 | 6.7 | 11.25 | 8.6 | 27.7 |
| 8.0 | 7.5 | 11.74 | 8.0 | 23.9 |

TABLE 2.3

Core Configuration and Composition

Fuel capsule
    Diameter [cm]                 1.5
    Wall thickness [cm]       0.05
    P/D                       1.5

Core Height [cm]             190.0 + 25 cm total reflector savings

Initial $^{240}$Pu/Pu           0.3

Volume Fractions
    Fuel (Pu-Co-Ce)       0.351
    Sodium               0.572
    Stainless Steel       0.025
    Tantalum             0.052

by the DPC code.[23]  Calculations were based on an assumed mid-cycle heavy atom burnup with atom densities of $^{239}$Pu, $^{240}$Pu, and fission product pairs (FPP) in the proportion

$^{239}$Pu:$^{240}$Pu:FPP::6:3:1.

The module (core plus blanket) used occupies the same total volume as that of the solid-fuel case (core plus blanket plus reflector).  Since the core region within each module occupies much less total volume than the solid-fuel core because of the omission of internal breeding material, a larger volume (1.7 times that in the Westinghouse case) is available for use as external blanket.

Table 2.4 summarizes the cases of interest and includes an estimate of the breeding ratio which would be appropriate to a finite (1000-MWe) system.  Breeding ratios comparable to those for the Westinghouse design are apparently achieved with no attempt at optimization. The use of the graphite reflector does not have a favorable effect in these cases.  It may also be noted that, while the seven-module case has some penalty in breeding relative to that for higher fuel densities, it is not unattractive, even in this unoptimized state.

The design and the model could still be greatly improved at this stage.  For example, the plutonium isotopic ratio and the effect of the axial blanket have been estimated by approximate methods.  The spatial variations of properties throughout the core and, more significantly, in the blanket have not been incorporated.  However, for the intended purpose of establishing a general range of economic potential and for investigating the effect of certain variants, these approximations are considered to be adequate.

TABLE 2.4

First-Round Estimates (1-D)

| Case | Number of Modules | $P_B$ [a] | $R_1$ [b] [cm] | $R_2$ [b] [cm] | Total Fissile Loading [kg] | Beginning of Life Fuel [g Pu/cc] | No. Modules for 1000 MWe | 1000-MWe $BR_{est.}$ |
|------|-------------------|-----------|----------------|----------------|----------------------------|----------------------------------|--------------------------|----------------------|
| 1 | ∞ | 0.25 | 27.0 | 71.8 | 2700 | 3.7 | 7 | 1.37 |
|   | 1 | 0.22 | 27.0 | 71.8 |      | 3.7 |   |      |
| 2 | ∞ | 0.26 | 24.2 | 60.4 | 3000 | 4.1 | 9.6 | 1.39 |
|   | 1 | 0.21 | 24.9 | 62.2 |      | 4.1 |     |      |
| 3 | ∞ | 0.29 | 18.1 | 45.1 | 3700 | 5.0 | 16.0 | 1.41 |
|   | 1 | 0.20 | 19.8 | 49.5 |      | 5.0 |      |      |
| 4 | ∞ | 0.30 | 13.1 | 32.8 | 4500 | 6.1 | 26.5 | 1.42 |
|   | 1 | 0.19 | 16.4 | 41.0 |      | 6.1 |      |      |
| Solid fuel[c] | ∞ | 0.18 | 41.2 | 71.8 | 3700 | | 7 | 1.49 |
|               | 1 | 0.12 | 41.2 | 71.8 |      | |   |      |

[a] $P_B$ is the blanket power fraction

[b] $R_1$ is the core radius [cm]; $R_2$ is the outer radius of the module [cm].

[c] The solid-fuel cases are similar to the two-dimensional cases reported in Ref. 11.

# 3. FUEL CYCLE COSTS

For simplicity in discussion, fuel cycle cost factors may be divided into four categories:

> fabrication, capitalization, and reprocessing
> inventory
> burnup and plutonium credit
> other costs.

The attempt throughout is to obtain cost estimates which may properly be compared with those of the reference solid-fuel case. Various aspects of the costing methods used here can thus be expected to suffer from the problems, if any, which may be identified in the solid-fuel study.[4]

It should be pointed out that the process line implied in the cost estimates for the liquid fuel is based on developed procedures. A significant quantity of reactor-grade nonrecycle fuel elements have been processed through all the steps indicated, for LAMPRE operations[21] and for extensive out-of-core testing. Detailed fabrication specifications have been prepared. The credit taken for volume production is small, and no credit is taken for process refinement.

The axial blanket is neglected in these cost calculations. The plutonium credit and the fabrication cost for this region are approximately equal. The radial blanket for the liquid-plutonium system has the same elements as does the solid-fuel system. However, the liquid-plutonium system employs nearly twice as many blanket elements as the solid-fuel system (56,500 vs 32,500).

One major cost consideration of a mixed (metal-core/refractory-blanket) system is that the metallic plutonium needed for makeup must be obtained from the nonmetallic fuel of the blanket. It is assumed that the oxide blanket will be reprocessed by aqueous methods. The output of this process must then be converted to metal. If an all-metal system were used (Section 5), this conversion charge would not be incurred.

24

Overhead cost estimates are based on those given in Ref. 8. The figures used are given in Table 3.1.

TABLE 3.1

Typical Annual Costs

|  |  | % of Direct Labor Charge |
|---|---|---|
| Equipment cost | $ 74,550 | 45.0 |
| Building cost | 36,900 | 22.3 |
| Direct labor | 165,567 |  |
| Indirect labor | 82,733 | 50.0 |
| Overhead & Maintenance Materials cost | 67,300 | 40.7 |
|  | $427,050 | 158.0 |

The in-core time (Appendix G) used for the reference case is approximately

$$t_{in-core} \approx \frac{(0.93 \cdot 10^3 [MWd/kgf])(BU[gf/cc])}{(SP_c [MW/kg])(\rho_c [g/cc])(F)} ,$$

where

$t_{in-core}$ = in-core time [d]

$BU$ = burnup [gf/cc]

$SP_c$ = reactor power/in-core inventory [MW/kg]

$\rho_c$ = density of plutonium in the core fuel [g Pu/cc]

$F$ = capacity factor [full-power days/day].

But since

$$SP_c = \frac{power}{fuel\ volume \cdot fuel\ density} = \frac{1.9 \cdot 10^3 [MW]}{(1.05 \cdot 10^3 [liter])(\rho_c [kg/liter])} ,$$

the in-core time for F = 0.8 and BU = 1.0 gf/cc is

$$t_{in-core} \approx \frac{(0.93 \cdot 10^3 [MWd/kgf])(1[gf/cc])(1.05[liter])}{(1.9[MW])(0.8)} = 650 \ [d].$$

(For comparison, see Section 4.1.)

## 3.1 Fabrication, Capitalization, and Reprocessing Costs

The fabrication basis used for the liquid-fuel core is outlined in Table 3.2. In estimating specific costs for this system, it is convenient to consider those costs associated with the fuel as separate from other fuel element fabrication costs. The fuel-independent fabrication costs are considered in Section 3.1.1; the fuel-dependent fabrication costs, in Section 3.1.2.

### 3.1.1 Capsule Manufacture

A simple fuel element design, with welded end caps, is assumed. Figure 3 shows one such design. The first phase of capsule production is the tubing procurement, fabrication, and carburization. It is assumed here that the capsule will have the selected cross section (1.5-cm o.d., 0.05-cm wall). The fueled length is specified as that of the solid-fuel case (190 cm). The total length, including the storage reservoir for volatile fission products, is 380 cm. This is estimated as being adequate to allow for the pressure stress limits associated with accumulation of volatile fission products (see Appendix E). It will be noted that the reservoir size does not depend on the density of the fuel used, for a specified burnup limit in terms of gf/cc.

The price of seamless high quality Ta-5W tubing of 1.5-cm diameter and 0.05-cm wall thickness is approximately $50/lb ($110/kg) plus $9/ft ($0.30/cm) for working and drawing to size. Thus, the material cost per capsule is

TABLE 3.2

Core Fabrication Cost Basis*

Fuel
    Material                          Pu-Co-Ce
    Plutonium content[g/cc]      3.7
    Fuel composition (w/o)
        Plutonium                 40.4
        Cobalt                    49.4
        Cerium                    10.2

Capsule
    Material                          Ta-5W
    Fuel region
        Length[cm]               190
        Outside diameter[cm]    1.5
        Wall thickness[cm]      0.05

    Gas space
        Length[cm]               190

Total Inventory
    Number of fuel elements     3591
        Plutonium content[kg Pu]  1.09 ea
        Fuel volume[liters]       $1.05 \cdot 10^3$

Other factors
    Plutonium burnup [gf/cc]    1.0
    Plant capacity factor       0.8
    Thermal efficiency          0.4

---

*Notes:  A combination of pyrochemical reconstitution in automated, shielded facilities, with aqueous recovery of residues, is assumed.

A fully developed process is assumed.

Recycle of cerium with the plutonium in the pyrochemical process, with a 20% makeup of as-purchased-and-filtered cerium, is used.

.022

.100 DIA.

FUEL LEVEL

24'-30°

13.0°

Fig. 3. Fuel Capsule

28
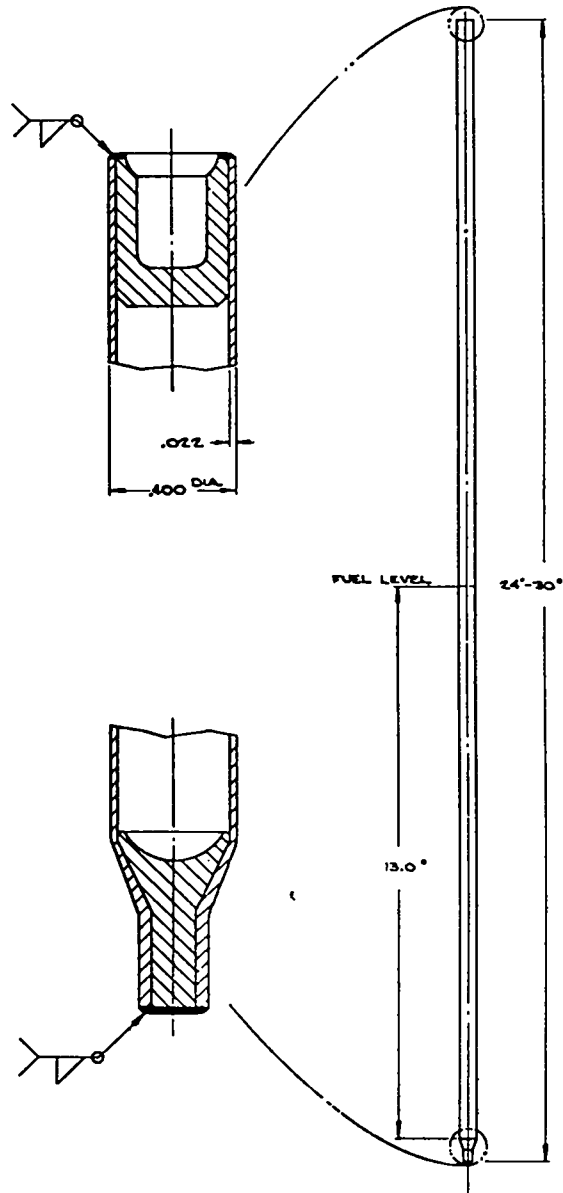
Weight of 380-cm tubing

$$= (16.6[\text{g/cc}])(\pi/4)(1.5^2 - 1.4^2[\text{cm}^2])(380[\text{cm/capsule}])$$

$$= 1.44[\text{kg/capsule}].$$

Tubing material cost

$$= (1.44[\text{kg/capsule}] \cdot 110[\$/\text{kg}]) + (380[\text{cm/capsule}] \cdot 0.30[\$/\text{cm}])$$

$$= \$272/\text{capsule}.$$

Fabrication of the tubing into capsules has been evaluated on the basis of individual operations and production of 3591 capsules in 650 days. The result of this evaluation is

$$\text{Fabrication cost} = 2 \text{ direct man-hours/capsule}$$
$$\text{Carburizing} = 0.5 \text{ direct man-hours/capsule}$$
$$\text{Total} = 2.5 \text{ direct man-hours/capsule}.$$

The cost is

$$(2.5[\text{DMh}])(5[\$/\text{hr}])(2.58[\text{overhead factor}]) = \$32/\text{capsule}.$$

Thus, the nonfuel capsule fabrication cost is \$304/capsule. Each capsule contains

$$(\pi/4)(1.4^2[\text{cm}^2])(190[\text{cm fuel/capsule}]) = 290[\text{cc fuel/capsule}].$$

Thus, at 1.0 gf/cc, there will have been 290 gf/capsule generated. Since there are 0.93 MWd/gf, this corresponds to

$$(290[\text{gf/capsule}])(0.93[\text{MWd/gf}]) = 270[\text{MWd/capsule}]$$
$$= 6.5 \cdot 10^6[\text{kWht/capsule}].$$

At a 40% thermal efficiency, $2.6 \cdot 10^6$ [kWhe/capsule] is obtained. Thus, the nonfuel fabrication of these capsules contributes

$$\frac{0.304 \cdot 10^6[\text{mil}]}{2.6 \cdot 10^6[\text{kWhe}]} = 0.12[\text{mil/kWhe (core)}].$$

29

This result must be adjusted to allow for the blanket power fraction; that is, the contribution to the total fuel cycle cost from core nonfuel fabrication is

$$0.12 \cdot P_c [\text{mil/kWhe}],$$

where $P_c$ is the core power fraction.

### 3.1.2  Fuel Fabrication, Capsule Loading, and Associated Costs

The fuel element costs associated with the fuel have been calculated in detail for the case described in Table 3.2.  A plutonium flow sheet for the fuel element fabrication and fuel reprocessing is shown in Fig. 4.  The costs inferred for this case, expressed as a cost per kilogram of plutonium in fabricated fuel elements, have been used for the (narrow) range of cases considered.  The average production rate is

$$\frac{3591 \text{ fuel elements}}{650 \text{ days}} = 5.5 \text{ fuel elements/day} \simeq \frac{6 \text{ kg Pu}}{\text{day}} .$$

At 95% yield, this means

6.3 kg Pu cast/day(average).

The plutonium batch size is limited by criticality considerations.  It is estimated that a 19-kg plutonium batch size of this alloy is safely below the criticality limit.  Thus, a single ingot per three-day period is indicated.

The number of direct-labor men required for work at eight hours per day is

| | |
|---|---|
| Cerium filtration and fuel casting, loading, hardness test, zone melting | 4 men |
| Chemical and spectrographic analysis | 2 " |
| X-ray and mechanical inspection | 1 " |
| Total | 7 men |
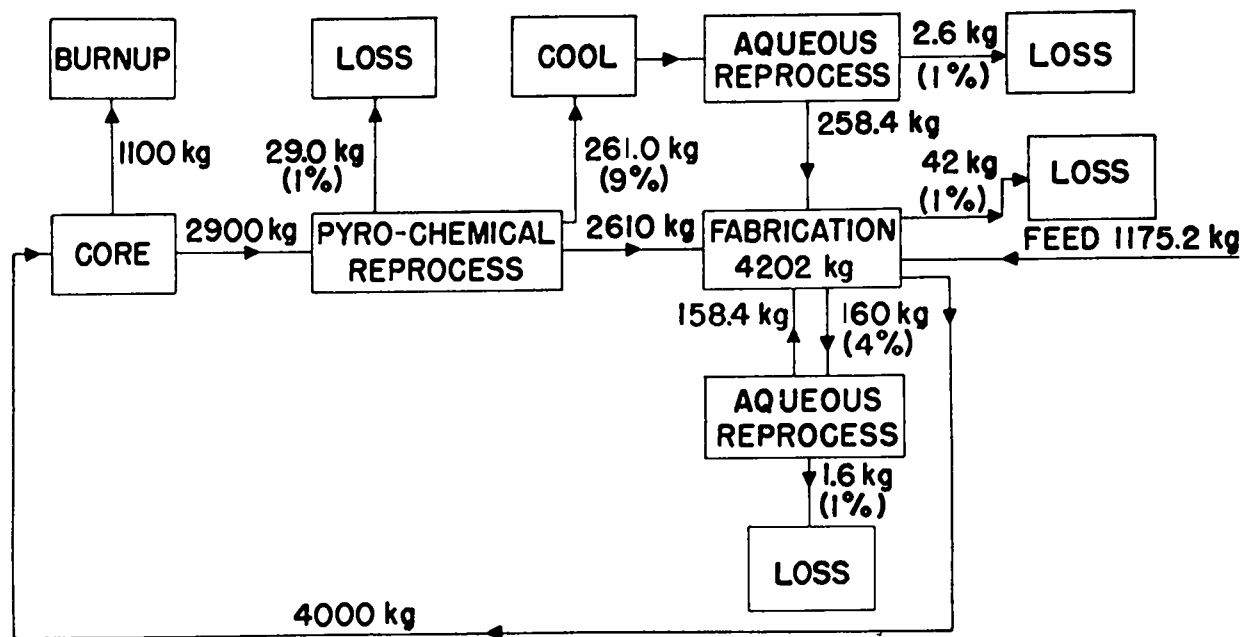
Fig. 4.  Flow Sheet for 1000-MWe Core Study

The work of these men for three days at eight hours per day corresponds
to

$$\frac{168[\text{direct man-hours}]}{19[\text{kg Pu}]} \simeq 8.8[\text{DMh/kg}].$$

Thus, the cost is

$$(8.8[\text{DMh/kg}])(5[\$/\text{DMh}])(2.58[\text{overhead factor}]) = \$114/\text{kg}.$$

The assumed 95% yield in casting is based on an allowance for 1% loss
and 4% recycle. The aqueous reprocessing cost, including a charge of
$\approx\$1.50/\text{g}$ for conversion to metal, is $\approx\$1900/\text{kg}$ (see below). Thus, the
4% recycle cost per kilogram fabricated is

$$\frac{1900[\$/\text{kg}] \cdot 0.04}{0.95} = \$80/\text{kg}.$$

The plutonium losses (see Fig. 4) of 1% in fabrication and 1% of the
recycle on reprocessing at a value assumed for plutonium of $\$10/\text{g}$ fissile,
or $\approx\$7/\text{g}$ plutonium, represent a cost of

$$\frac{(7000[\$/\text{kg}])(0.01 + 0.04 \cdot 0.01)}{0.95} = \$74/\text{kg}.$$

Additional material costs are

      Cerium cost = $38/kg Pu based on 20% replacement after chemical
                          processing

      Cobalt cost = $2/kg Pu

$$\frac{\text{Feed conversion}}{\text{Charge}} = \frac{\text{kg Pu feed} \cdot \$1500/\text{kg conversion cost}}{\text{kg Pu in product}}$$

$$= \frac{(1175[\text{kg}])(1500[\$/\text{kg}])}{4000[\text{kg}]}$$

$$= \$440/\text{kg}.$$

The fuel-dependent fabrication costs per kilogram of plutonium in fabricated fuel elements are summarized in Table 3.3.

TABLE 3.3

Fuel-Dependent Fabrication Costs

|  | Cost/kg Pu |
|---|---|
| Fuel casting and capsule loading | $114 |
| Waste and cropping recycle | 80 |
| Plutonium loss | 74 |
| Cerium cost | 38 |
| Cobalt cost | 2 |
| Feed conversion | 440 |
| Total | $748/kg Pu |

To relate this to cost per kilowatt-hour [mil/kWhe], consider the total energy output per core cycle. The total energy output per cubic centimeter of core fuel at 40% thermal efficiency is

$$\frac{1[gf/cc] \cdot 0.93[MWd/gf]}{P_c} = \frac{0.93}{P_c}[MWd/cc] = \frac{8.9 \cdot 10^3}{P_c}[kWhe/cc \ fuel].$$

The total fuel-dependent fabrication cost per cubic centimeter of fuel in the core is $\rho_c \cdot \$0.75$. The contribution to the fuel cycle cost then becomes

$$\frac{0.75 \cdot 10^3 \ \rho_c[mil/cc \ fuel]}{8.9 \cdot 10^3/P_c[kWhe/cc \ fuel]} = 0.084 \ \rho_c \ P_c[mil/kWhe].$$

### 3.1.3  Working Capital

In the solid-fuel study,[4] interest on fuel fabrication is computed at 6% per year on book value. The book value is assumed to decrease linearly to zero over the in-core residence time. Assuming simple interest, the above represents 6% on one-half the total fabrication cost. The total working capital charge is then 3% of the cost for fabrication, excluding the plutonium feed conversion cost.

### 3.1.4 Spent-Fuel Reprocessing

A combination aqueous and pyrochemical process is specified for spent-fuel reprocessing. Extensive work has been done on both of these processes. Pyrochemical development work has been done both relative to EBR-II-type fuel[20] and directly on the liquid alloy fuels.[24] Procedures for electrorefining these fuels have also been successful.[25,26] It is not possible at this stage to establish quantitatively the difference in costs for the two processes. Either process is clearly feasible and is developed to the point at which a pilot plant could be designed.

Pyrochemical processing is estimated to cost between \$150 and \$200/kg Pu. An aqueous process would be used to process an estimated 9% carry-over from the pyrochemical processing. The estimated process cost is \$1.90/g, about \$0.40 for the aqueous steps and about \$1.50 for the conversion of the end product to metal. Thus, the cost per kilogram of residual plutonium is

$150 to $200/kg for the pyrochemical processing
+ 0.09 · $1900/kg for the aqueous processing

= $320 to $370/kg residual plutonium.

The number used in further calculations will be \$345/kg residual plutonium.

Plutonium losses incurred in the above processing are charged as

$$\left\{ \begin{array}{c} 1\% \text{ loss in pyrochemical} \\ \text{reprocessing} \end{array} + \begin{array}{c} 1\% \text{ loss in aqueous} \\ \text{reprocessing} \end{array} \right\} \cdot \$7000/\text{kg fissile Pu},$$

$$\{0.01 + (0.01 \cdot 0.09)\}[\text{kg/kg residual Pu}] \cdot 7000[\$/\text{kg}] = \$76/\text{kg}$$
$$\text{residual Pu.}$$

The total is then

$345/kg + $76/kg = $421/kg residual Pu.

The contribution to the fuel cycle cost is

$$\frac{(\$/kg~residual~Pu)(kg~residual~Pu)}{power~output}$$

$$= \frac{(\$/kg~residual~Pu)(end\text{-}of\text{-}life~fuel~density)(fuel~volume)}{BU \cdot (kWhe/gf)(fuel~volume)} ~.$$

At 40% thermal efficiency, this is

$$\frac{(421[\$/kg~residual~Pu])~(\rho_c - 1.0)[kg~residual~Pu/liter]}{(8.9 \cdot 10^3/P_c[kWhe/cc~fuel])}$$

$$= 0.047(\rho_c - 1)~P_c[mil/kWhe] ~.$$

### 3.2  Plutonium Inventory Charges

The inventory charge for core plutonium is a direct function of core fissile loading (for a given power). With a 10% inventory charge rate, this can be written as

Active Pu inventory charge =

$$\frac{10^4 \left[\dfrac{\$}{kg~fissile}\right] 0.1[Annual~interest~rate]~L[kg~Pu~in~core]~\epsilon\left[\dfrac{kg~fissile}{kg~Pu}\right]}{365\left[\dfrac{d}{yr}\right] 2500[MWt]~24\left[\dfrac{h}{d}\right] 0.4\left[\dfrac{MWe}{MWt}\right] 0.8[load~factor]} ~.$$

For $\epsilon = 0.7$, this becomes

active Pu inventory charge $= 10^{-4}~L[mil/kWhe] = 10^{-4}~V_F~\rho_c$

where

$V_F$ is the core fuel volume,

$\rho_c$ is the plutonium density in the fuel.

Since there are $1.05 \cdot 10^3$ liters of fuel volume, this can also be written as

Active Pu inventory charge $= 10^{-4} \cdot 1.05 \cdot 10^3 \cdot \rho_c \frac{mil}{kWhe} = 0.105 \, \rho_c \frac{mil}{kWhe}$ .

The inactive inventory is conveniently related to the in-core inventory. As shown in Appendix G (Eq. G.9), the inventory ratio may be expressed as

$$\frac{\text{out-of-core inventory}}{\text{in-core inventory}} \simeq \frac{(t_{out}[d])(SP_c[MW/kg])(F)(\rho_c[g/cc])}{(0.93 \cdot 10^3 [MWd/kgf])(BU[gf/cc])} .$$

With $F = 0.8$, this can be written

$$\frac{\text{out-of-core inventory}}{\text{in-core inventory}} =$$

$$\frac{(t_{out}[d]) \left( \dfrac{p[MW] \cdot P_c}{V_F[\text{liters}] \, \rho_c[\text{kg/liter}]} \right)(0.8)(\rho_c[g/cc])}{(0.93 \cdot 10^3 [MWd/kgf])(BU[gf/cc])}$$

where

   $p$ is the reactor power

   $P_c$ is the core power fraction.

For $p = 2500$ MWt, this is

$$\frac{2.15 \cdot P_c \cdot t_{out}}{V_F} .$$

For the present case, this becomes

$$\frac{\text{out-of core inventory}}{\text{in-core inventory}} = 1.56 \cdot 10^{-3} \, t_{out}.$$

For $t_{out}$ = 100 days (for the assumed processing setup, the out-of-core time will probably be significantly less than this),

$$\frac{\text{out-of-core inventory}}{\text{in-core inventory}} \approx 0.16.$$

Thus, the total inventory charge is

$$0.105 \; \rho_c(1 + 0.16)[\text{mil/kWhe}] = 0.122 \; \rho_c[\text{mil/kWhe}].$$

## 3.3  Burnup and Plutonium Credit

A gross burnup (BU) charge is obtained from

$$\frac{10^3[\text{mil/\$}] \cdot 10[\text{\$/gf}]}{24[\text{h/d}] \cdot 0.4[\text{MWe/MWt}] \cdot 0.93[\text{MWd/gf}] \cdot 10^3[\text{kW/MW}] \cdot 1/P_c[\text{MW/MW(core)}]}$$

$$= \frac{10^4 \cdot P_c}{8.9 \cdot 10^3}[\text{mil/kWhe}] = 1.12 \; P_c[\text{mil/kWhe}].$$

When applied to the entire reactor, this may be corrected by a fission contribution from fertile material of $\approx 20\%$. Thus, the gross BU charge may be estimated to be

$$\text{BU charge} \cdot 0.90 \; P_c[\text{mil/kWhe}].$$

To a first order approximation, the plutonium credit may be estimated as

$$\text{Pu credit} \approx \text{BR} \cdot \text{BU charge}$$

where BR is the reactor breeding ratio. The net plutonium charge is thus $(1 - \text{BR}) \cdot 0.90 \; P_c[\text{mil/kWhe}]$.

37

## 3.4 Miscellaneous

The figures used in the solid-fuel report[4] are considered to be appropriate for all other costs, except as noted.

### 3.4.1 Shipping

On-site preliminary processing is assumed. The associated cost is

$$\text{Shipping cost} = \frac{(\$/kg \text{ for shipping})(\text{core fraction shipped})}{(\text{thermal efficiency})(BU[gf/cc]/\rho_c)(MWdt/gf)(kWh/MWd)} \cdot$$

Using the following factors:

$50/kg shipping cost[4]
0.1 core fraction shipped
0.4 thermal efficiency
1.0 g Pu/cc burnup
0.93 MWdt/gf
$\rho_c \simeq 4$ g Pu/cc fuel

$$\text{shipping cost} = \frac{(50[\$/kg])(0.1)}{(0.4[MWe/MWt])(1.0/4.0[gf/g])(0.93 \cdot 10^3[MWd/kgf])(24[h/d])}$$

$$= 0.002[mil/kWhe].$$

### 3.4.2 Axial Blanket

The axial blanket of the solid-fuel core is at both the top and bottom of the core, whereas the axial blanket for the liquid Pu-Co-Ce alloy core is only at the bottom. The fabrication and reprocessing costs for the axial blanket of the solid-fuel case total 0.036 mil/kWhe, and there is an 0.052 mil/kWhe plutonium credit.[4] Based on these numbers, it was felt that the axial blanket could be neglected in this estimate on the liquid Pu-Co-Ce alloy core.

### 3.4.3  Radial Blanket

The fuel cycle costs associated with the blanket can be established relative to those for the solid-fuel study.  Since the blanket fuel elements are taken to be those selected by Westinghouse,[4] it is reasonable to assume that most costs per element will be independent of the type of core element used, provided the total blanket burnup is comparable.  These costs would include fabrication, reprocessing, and inventory.  The only likely differences would be in the costs associated either with fuel management or with a different thermal rating, but there is no reason to expect even those costs to be significantly higher for the liquid-fuel core than for the solid-fuel core.  Thus, we may consider the total cost per blanket element to be the same for both cases.

The core power per blanket element cannot be predicted in detail without a detailed life history study.  However, it is possible to obtain a reasonable estimate of an average residence time.  In Appendix H, an estimate is given of the blanket burnup per core cycle.  From the figures given in Appendix H, it is seen that the blanket in the liquid-fuel case has a burnup per core cycle of only about one-third that of the solid-fuel case.

The time in-core, and therefore core total energy output per cycle, may be obtained (see Appendix G) from:

$$
\frac{(BU[gf/cc])(0.93 \cdot 10^3 [MWd/kgf])}{(SP_c[MW/kg])(\rho_c[g/cc])}
$$

$$
= \frac{(BU[gf/cc])(0.93 \cdot 10^3 [MWd/kgf])(L[kg])}{(p_c[MW])(\rho_c[g/cc])}
$$

$$
= \frac{0.93 \cdot 10^3 \, BU \cdot L_f}{p_c \rho_f} [\text{full power days}],
$$

where

BU is burnup [gf/cc]

$SP_c$ is active core specific power [MW/kg]

$\rho_f$ is fissile density in core [gf Pu/cc]

$p_c$ is core power {1900 MWt}

$L_f$ is fissile loading [kg]

For the cases considered, we may infer a ratio of in-core times of

$$\frac{t_{in-core}^{liquid}}{t_{in-core}^{solid}} = \frac{BU^{liquid}}{BU^{solid}} \ \frac{L_f^{liquid}}{L_f^{solid}} \ \frac{\rho_f^{solid}}{\rho_f^{liquid}} \ \frac{p_c^{solid}}{p_c^{liquid}} \simeq 1 \cdot 0.7 \cdot 0.5 \cdot 1.0 = 0.35.$$

From the dimensions considered (Table 2.4), the ratio of blanket areas, and thus of the number of blanket elements, is

$$\frac{N^{liquid}}{N^{solid}} \propto 1.7 \ .$$

Thus, for three blanket cycles per core cycle, the relative radial blanket cost is

$$\frac{\text{relative cost per element} \cdot \dfrac{N^{liquid}}{N^{solid}}}{\text{relative time per core cycle} \cdot \text{relative blanket cycles/core cycle}}$$

$$= \frac{1 \cdot 1.7}{0.35 \cdot 3} \simeq 1.7.$$

## 3.5  Summary of Factors

The cost factors obtained for the liquid-fuel case are summarized in Table 3.4.

TABLE 3.4

Cost Factor Summary

Fabrication and Reprocessing Costs:

| | |
|---|---|
| Capsule manufacture | $= 0.12 \cdot P_c$ [mil/kWhe] |
| Fuel fabrication, etc. | $= 0.084 \; \rho_c \; P_c$ [mil/kWhe] |
| Working capital | $= 0.03 \cdot$ fabrication |
| Spent fuel processing | $= 0.047 \; (\rho_c - 1) \; P_c$ [mil/kWhe] |

Plutonium inventory charge $= 10^{-4} \; V_F \rho_c \left\{ 1 + \dfrac{215}{V_F} \; P_c \right\}$ [mil/kWhe]

Net plutonium charge $= (1 - BR) \cdot 0.90 \; P_c$ [mil/kWhe]

Miscellaneous

| | |
|---|---|
| Shipping | $= 0.002$ [mil/kWhe] |
| Axial blanket | $=$ nil |
| Radial blanket | $= 1.7 \cdot$ solid-fuel case |

## 3.6  Application to Specific Cases

The specific cases considered in Section 2 have been used to evalu-
ate the fuel cycle costs.  The Westinghouse figures are based on those
from the reference solid-fuel case[4] with the following exceptions:  A
use charge rate of 10% rather than 4.75% is used, and the net plutonium
charge is based on the figures from Section 3.2.  The summary costs are
listed in Table 3.5.  For this table, the solid-fuel case was described
with the analytic techniques that were used for the liquid-fuel cases.

There is no feature of the liquid-plutonium system which is signi-
ficantly out of line with those of the Westinghouse case.  Presumably,
there are economies which may be available in either type of system.
There is no indication that any other solid-fuel system has significantly
better costs than those predicted for the solid-fuel case (in fact, these
costs are among the best claimed for any solid-fuel system).[11]  By
inference, the liquid-plutonium system can also be expected to be generally
competitive in costs.  It is also observed that the seven-module case is
as good as, or better than, any of the other cases considered.  Section 5
includes a discussion of the cost implications of a more fully optimized
liquid-plutonium system.

TABLE 3.5

Reference Fuel Cycle Cost Estimates
[mil/kWhe]

| | Solid Fuel | Liquid Fuel | | | |
|---|---|---|---|---|---|
| Number of modules | 7 | 7 | 9.6 | 16.0 | 26.5 |
| Plutonium density [g Pu/cc fuel] | | 3.7 | 4.1 | 5.0 | 6.1 |
| Fabrication costs[a] | 0.21 | | | | |
|    Fuel-independent | | 0.09 | 0.09 | 0.09 | 0.09 |
|    Fuel-dependent | | 0.23 | 0.26 | 0.32 | 0.38 |
| Working capital | 0.01 | 0.01 | 0.01 | 0.01 | 0.01 |
| Reprocessing[a] | 0.12 | 0.09 | 0.11 | 0.14 | 0.18 |
| Plutonium inventory[b] | 0.68 | 0.45 | 0.50 | 0.61 | 0.74 |
| Shipping | 0.01 | nil | nil | nil | nil |
|    Subtotal | 1.03 | 0.87 | 0.97 | 1.17 | 1.40 |
| Radial blanket | 0.24 | 0.41 | 0.41 | 0.41 | 0.41 |
|    Subtotal | 1.27 | 1.28 | 1.38 | 1.58 | 1.81 |
| Net plutonium cost | (0.38) | (0.25) | (0.26) | (0.28) | (0.29) |
|    Net total | 0.89 | 1.03 | 1.12 | 1.30 | 1.52 |

---

[a] Including losses.

[b] At 10% inventory charge rate.

## 4. PERFORMANCE DESCRIPTION

Although the arrangement considered is not intended as a specific proposal and certainly does not reflect a fully evaluated design, it is of some interest to consider a few of the operating characteristics of such a system. Many of the general properties would be similar for a wide range of cases. Four aspects are considered here:

(1) The implied fuel cycle and control requirements,
(2) Power distributions and power shifts with time,
(3) Unique features associated with the fluidity of the cycle, and
(4) Reprocessing.

In each case, the treatment is illustrative rather than exhaustive.


### 4.1  Fuel Cycle

One of the major changes in viewpoint required in discussing this type of system relative to the more common approaches is that associated with total external breeding. A well-known advantage of a breeder system is that the reactivity loss rate associated with burnup is lessened by the production of fissile material. It is tempting to assume that, since the reactivity of an external breeder is controlled by the driver (core), the reactivity drift of the system is that of a burner system. This is clearly wrong, because even though there will be a shift in reactivity from core to blanket, the increased plutonium in the system partially compensates for the core reactivity loss. In fact, if the worth of neutrons born in the blanket were high enough, a reactivity increase would occur.

In order to illustrate this and other features of the comparative fuel cycles, a set of one-dimensional $S_n$ depletion calculations has been done, using the DTF-BURN code.[27] For each fuel type, depletion calculations for the single-module and for the infinite-array cases were

performed. The beginning-of-life compositions and dimensions used are given in Table 4.1. The compositions were selected in such a way that mid-life compositions would be similar to those used in Section 2.4. It should be noted, however, that no attempt is made to obtain a precise correspondence with previously described calculations.

The solid-fuel case is described as using a simple batch loading both in core and blanket. The blanket life is assumed to be determined by the core and not by any internal limitations. A poison (tantalum) control is used.

The liquid-fuel case similarly uses a single-batch loading for the core. However, the blanket burnup is substantially less per core cycle than for the solid-fuel core (see Appendix H). Thus, for similar blanket properties, it is reasonable to use partial blanket reloads. In the case considered here, one-third of the blanket (scatter refueling) is replaced at each core replacement. The beginning-of-cycle blanket atom densities used are based on the estimated blanket depletion per cycle as discussed in Appendix H. A poison control is again assumed.

There are several significant representational differences between these depletion cases and the cases considered in Section 2. In particular, the compositions differ somewhat, and the Mills[28] cross-section library is used rather than the Hansen-Roach set.[15] The most significant difference is the use of poison control for the liquid-fuel case, whereas in Section 2 a fuel control element was assumed. Thus, a detailed comparison of these cases with the cases considered previously is likely to be misleading. The comparison between the liquid-fuel and the solid-fuel cases should still be meaningful, if the cases compared use the same representation.

The no-control reactivities obtained from these calculations are given in Table 4.2. It is seen that for the poison control case, the liquid-fuel reactivity loss is significantly more than for the solid-fuel case. The rate of reactivity loss per percentage fuel burnup, however, is comparable.

44

## TABLE 4.1

### Burnup Study Inputs

| Nuclides | Atom Densities | | | | |
|---|---|---|---|---|---|
| | Solid-Fuel Case | | | Liquid-Fuel Case | |
| | Core | Blanket | Reflector | Core | Blanket |
| Iron | 0.009142 | 0.0118 | 0.002949 | 0.0015 | 0.0118 |
| Chromium | 0.002351 | 0.003033 | 0.0007582 | 0.00039 | 0.003033 |
| Nickel | 0.001470 | 0.001897 | 0.0004741 | 0.000228 | 0.001897 |
| Sodium | 0.01184 | 0.005372 | 0.00108 | 0.01227 | 0.005372 |
| Oxygen | --- | 0.0238796 | --- | --- | 0.0238796 |
| Carbon | 0.0094053 | --- | 0.072 | --- | --- |
| $^{235}U$ | --- | 0.0000358 | --- | --- | 0.0000175 |
| $^{238}U$ | 0.007265 | 0.011904 | --- | --- | 0.011471 |
| $^{239}Pu$ (a) | 0.0014982 | --- | --- | 0.002469 | 0.0003554 |
| $^{240}Pu$ (b) | 0.0006421 | --- | --- | 0.001058 | 0.0000050 |
| FP atoms | --- | --- | --- | --- | 0.0000839 |
| Tantalum | --- | --- | --- | 0.0028756 | --- |
| Cobalt | --- | --- | --- | 0.003352 | --- |
| Cerium | --- | --- | --- | 0.0066233 | --- |
| Outer Radius [cm] | 41.91 | 65.56 | 71.76 | 27.02 | 71.76 |

(a) Represents total fissile plutonium [$^{239}Pu$ + $^{241}Pu$]

(b) Represents total nonfissile plutonium [$^{240}Pu$ + $^{242}Pu$]

## TABLE 4.2

### No-Control Eigenvalues
### (Poison Control)

| Solid Fuel | | Liquid Fuel | |
|---|---|---|---|
| Burnup [gf/cc] | K | Burnup [gf/cc] | K |
| 0 | 1.097 | 0 | 1.177 |
| 0.05 | 1.091 | 0.04 | 1.171 |
| 0.11 | 1.087 | 0.11 | 1.157 |
| 0.21 | 1.078 | 0.22 | 1.137 |
| 0.43 | 1.062 | 0.43 | 1.098 |
| 0.75 | 1.041 | 0.63 | 1.061 |
| 1.17 | 1.021 | 0.82 | 1.027 |
| | | 0.95 | 1.006 |

The choice of a control system also has a strong effect on the breeding potential of the system. Table 4.3 lists the radial breeding factors (see Appendix A for definition) for two alternative methods of controlling the liquid system (no allowance is made for axial blanket in either case). The poison control case is that described above. The case labelled "Fuel Control" is maintained at critical by adjusting the position of the boundary between core and blanket to represent the insertion or removal of peripheral fueled control elements. It may be noted that this representation is not particularly realistic, in that the material inserted into and removed from the control zone has the average composition of the corresponding zone. These data indicate that a poison control in this system could reduce the breeding ratio, relative to moving fuel control, by an average over the cycle of 0.3. For either of these cases, the control requirement for burnup can be reduced by partial refuelings. With a moving fuel control system, the control elements are likely to be overcooled when they are removed from the core. This excess flow adds to the allowance required for the core-to-blanket power shift.

Some factors of the two fuel cycles are given in Table 4.4. Any of these factors can be changed by design with, of course, some corresponding changes in other factors. The burnup limits in both cases are selected arbitrarily. The design variations for the solid-fuel cases are not considered here but involve an interaction among fuel enrichment, specific power, breeding, and fabrication costs.

The time per cycle for the liquid fuel is somewhat flexible. Using a burnup limit based on fission product density, the total energy, and thus time per cycle, can be changed by changing the fuel volume. This can be compensated for by a change in plutonium concentration in the fuel.

Unfortunately, with a container having a high cross section and a moderating blanket, there is only a modest range available prior to a need for a re-optimization among breeding and specific power. It may be

TABLE 4.3

Effect of Control Method

| Poison Control | | Fuel Control | |
|---|---|---|---|
| Burnup [gf/cc] | Radial Breeding Factor | Burnup [gf/cc] | Radial Breeding Factor |
| 0 | 0.82 | 0 | 1.47 |
| 0.11 | 0.88 | 0.16 | 1.45 |
| 0.22 | 0.92 | 0.32 | 1.42 |
| 0.43 | 1.02 | | |
| 0.63 | 1.12 | 0.58 | 1.38 |
| 0.82 | 1.22 | 0.80 | 1.33 |
| 0.95 | 1.28 | 1.00 | 1.29 |


TABLE 4.4

Fuel Cycle Factors

| | Solid Fuel Case | Liquid Fuel Case |
|---|---|---|
| **Core** | | |
| Burnup limit | 100[MWd/kg] ($\approx$1.2[gf/cc]) | 1[gf/cc] |
| Time cycle | | |
| Full power days | 1100 | 580 |
| Days at 80% load factor | 1400 | 725 |
| Peak burnup | | |
| Peak capsule | 150[MWd/kg] | 1.4[gf/cc] |
| Peak point | 220[MWd/kg] | |
| **Blanket** [a] | | |
| Peak burnup | 0.15[gf/cc] | 0.25 [b] |
| Average burnup | 0.06[gf/cc] | 0.08 [b] |
| Average Pu content at end of exposure | 3.2% | 3.9% [b] |

---

[a] Assumed to be nonlimiting.
[b] Estimated as property at end of three-core cycles.

noted that changes in the number of fuel elements in the system do not change the fabrication cost (in mil/kWhe). For the example given, it might be desirable to go to a one-year cycle. If this were done in conjunction with a half-refueling, some advantage might be gained in such factors as blanket peaking and control required.

## 4.2  Power Distribution

There are three factors which determine the major features of the power distribution: The relative power distribution among the modules, the power swing with burnup, and general hot-spot factors. The effect of control element motion is not a major perturbation, but some allowance for this may be made.

In any modular system, the peaking will be greater than that in a homogeneous system, because of the localization of the fissile material in the core regions. Table 4.5 lists the core and blanket radial peaking factors obtained for the reflected cells. For a uniform core, the radial peaking factor is generally ≃1.3. Table 4.6 lists the power fractions for the various times in life. With regard to engineering factors, several comments may be made in comparison of the cases. In general, the smaller the dimensions, the more severe the effects of local toler-ances are likely to be. Thus, the larger capsules associated with the liquid fuel permit looser tolerances. The larger P/D ratio also favors the liquid fuel in that it will yield a reduced azimuthal temperature variation. In addition, the elimination of straining of the fuel ele-ments from fuel swelling and thermal expansion (e.g., bowing) removes a major cause of nonuniform power distributions.

Thus, it may be concluded that the total thermal design allowances for the two systems will be comparable, except for the generally higher blanket power level in the liquid-fuel case.

48

TABLE 4.5

Peak-to-Average Powers[a]

| | Solid Fuel Case | | Liquid Fuel Case | |
| | Core | Blanket | Core | Blanket[b] |
|---|---|---|---|---|
| Beginning-of-life | 1.55 | 2.8 | 1.52 | 3.5 |
| Mid-life | 1.50 | 2.4 | 1.39 | 3.3 |
| End-of-life | 1.40 | 1.9 | 1.20 | 3.1 |

[a] Single compositions only are described for core and blanket. Thus, only relative values are of particular significance.
[b] Single core cycle; three-cycle scatter blanket fueling.


TABLE 4.6

Blanket Power Fractions

| | Solid Fuel Case | Liquid Fuel Case[a] |
|---|---|---|
| Beginning-of-life | 4% | 18% |
| Mid-life | 10 | 26 |
| End-of-life | 21 | 37 |

[a] Single core cycle; three-cycle scatter blanket fueling.

49

## 4.3  Fuel Circulation and Bubbles

One of the unique features of a liquid-fuel system is the need to consider the dynamics of the fuel itself.  In this connection, two particular questions which may be raised relate to the effects of natural convection within the fuel and to the accumulation and release of bubbles of volatile fission products.

The rate of convection has been estimated, using Murgatroyd's methods.[29]  Murgatroyd assumes uniform volumetric heat source; zero axial temperature gradiant; fluid fuel in a vertical tube which is long enough to exhibit fully developed convective flow in its central section, to which his attention is confined; Prandtl numbers in the range 0.01 to 1.00; and eddy coefficients of heat and momentum as measured at California Institute of Technology.[30]  Because Murgatroyd's cases were few, it has been necessary to interpolate.

Flow characteristics are estimated for two cases:  one in which the flow is assumed to be laminar, and one in which the flow is assumed to be turbulent.  Reynolds numbers, based on the central velocity and the diameter of the rising stream, are then used to determine which type of flow is appropriate.  On the basis of experiments by Onsager and Watson[31] on a thermal diffusion column and a discussion by Woodrow,[32] onset of turbulence is assumed to occur at a Reynolds number of about 50.  While it is not clear that the lengths of interest here are sufficient to attain the fully developed flow assumed by Murgatroyd, estimates made on that basis are useful because the severity of convective effects will be overestimated.  A summary of input data and calculational results is given in Table 4.7.  These results indicate that the convective flow is likely to be turbulent, with centerline velocities of about 5 cm/sec.

One consequence of fuel convection is a net upward heat transport which adds to the heat flux near the top of the fuel.  However, the heat transported upward by convection is moderate, being equal to that generated in a section of capsule whose length is less than half a radius.  It is reasonable to assume that the convected heat flows out at the top of

50

TABLE 4.7

Estimated Convective Effects

A. Assumed Input Data

| | | |
|---|---|---|
| Core power | [MWt] | 1900 |
| Nominal fuel | [g Pu/cm$^3$] | 3.3 |
| Assumed average temperature | [°C] | 870 |
| Fuel radius | [cm] | 0.711 |
| Fuel height | [cm] | 190.5 |
| Fuel density | [g/cm$^3$] | 8.7 |
| Volume expansion coefficient | [°C$^{-1}$] | 90 x 10$^{-6}$ |
| Thermal conductivity | [W/cm-°C] | 0.20 |
| Viscosity (poise) | [g/cm-sec] | 0.044 |
| Kinematic viscosity | [cm$^2$/sec] | 0.0051 |
| Specific heat | [W-sec/g-°C] | 0.37 |
| Thermal diffusivity | [cm$^2$/sec] | 0.062 |
| Prandtl number | | 0.080 |
| Average power density | [W/cm$^3$] | 1800 |
| Modified Grashoff number | | 5.54 x 10$^6$ |

B. Results, Assuming Fully Developed Laminar Flow

| | | |
|---|---|---|
| Centerline temperature (over wall)($T_c$) | [°C] | 1140 |
| Centerline velocity ($v_c$) | [cm/sec] | 206 |
| Reynolds number | | 15000 |

C. Results, Assuming Fully Developed Turbulent Flow

| | | |
|---|---|---|
| $T_c/T_c$ (laminar) | | 0.48 |
| $v_c/v_c$ (laminar) | | 0.026 |
| Centerline temperature (over wall)($T_c$) | [°C] | 550 |
| Centerline velocity ($v_c$) | [cm/sec] | 5.4 |
| Reynolds number | | 380 |

the fuel through a section of the capsule wall whose length is about one radius. The conducted heat in this region is low, because of the normal axial flux distribution. The heat flux in this top section from conductive and convective effects combined is calculated to be less than the average heat flux in the core. Another consequence of the fuel convection is the potential enhancement of mass transfer of the wall material by the fuel.

The second question raised by the use of a liquid fuel concerns the growth and release of bubbles of gaseous fission products. Experience with LAMPRE[21] indicated that during operation at power the bubbles accumulate, mainly on the capsule walls, until a saturation volume of approximately 4.5% of the fuel volume is attained. This bubble content of the fuel and the associated reactivity were quite stable against short-term fluctuations, and no deleterious effect was ever attributable to these bubbles. On the other hand, calculations have indicated[21] that the presence of bubbles could act as a cushion to reduce the peak pressures generated within the fuel during hypothetical reactivity excursions.

Compared to LAMPRE, the escape of bubbles should be facilitated by the larger diameter capsules (1.4 cm vs 0.95 cm i.d.) and the higher convective velocity (5.4 vs 1.8 cm/sec) of this study. On the other hand, the longer fuel column (190 cm vs 15 cm) and higher volumetric gas generation rate (1.8 vs 0.7 MW/liter) should favor higher volumetric gas retention in the fuel.

Although moderate and reasonable extrapolations from past experience lead to optimism in regard to dynamic effects in the fuel of the present proposal, it is clear that further fuel irradiation experiments are needed to evaluate these effects adequately.


4.4 Reprocessing

The economic estimates used (Section 3) specifically assume that pyrochemical reprocessing is to be employed. This should not be taken to imply that such a process has been fully developed. It is easily

shown, however, that an aqueous processing scheme, using presently available costs, is unattractive. This is clear from the costs for the 90% pyrochemical processing relative to those for the 10% aqueous processing. Each of these parts contributes approximately the same amount to the total costs (see Section 3.1.4), while the unit costs differ by an order of magnitude.

Much work has been done in pyrochemical processing, and a process based on that used for EBR-II[20] may be useful. Flow sheets have been sketched which indicate possible nonaqueous sequences, but at this stage it is not feasible to select a reference process or to defensibly estimate costs, decontamination factors, or yields for such processes.

An alternative method for reprocessing these fuels may be available in electrorefining, on which sufficient work has been done to define processes of potential interest.[25] Associated costs are reported to be reasonable relative to those predicted for other methods.

Two other factors in reprocessing should be noted. First, there may be a reprocessing incentive to use a recycled fuel which differs chemically from the ternary alloy which has been investigated to date; that is, it may be attractive to leave certain of the fission products in the fuel. Neither the economic nor the materials implications of such an alternative have been thoroughly investigated. Secondly, the normal fluidity of the fuel may allow certain simplifications. The volatile fission products can be removed mechanically at whatever stage is most convenient. Certain other fission products will precipitate in the core and can be discarded with the capsule. It has been suggested that a decay heat liquation step might be effective in removing some fission products. The combination of these factors may permit some shortening of the normal reprocessing sequence.

# 5.  DESIGN VARIANTS

## 5.1  More Optimistic Case

The deliberately conservative assumptions of Section 3 may give an unduly pessimistic view of the near-term fuel cycle cost potential of a system using a liquid-plutonium-fuel core.  Therefore, a comparison case is considered in which the following changes of assumed limits are used:

(1)  Thin (0.03 cm) container wall
(2)  Vent tube release of fission products to the cover gas
(3)  Solid-metal blanket
(4)  Use of nonaqueous methods for all processing, including skull and scrap recovery
(5)  Increased assumed processing yields.

No attempt has been made to obtain an optimum design for this revised basis.  In particular, with a solid-metal blanket, it may be that that an internal breeding arrangement would be preferable.  Further, no attempt has been made to evaluate the performance requirements that this concept would place on the blanket.  Thus, the present data should be used only as an indication of the potential cost reduction.  Features beyond those indicated in previous studies would require demonstration.

The blanket rod size assumed is the same as was used for the oxide blanket of the solid-fuel case (1.2 cm o.d. rods with 0.05 cm stainless steel clad).  In this case, however, a metal alloy fuel is assumed. Neither fabrication nor reprocessing costs are estimated for the blanket.

The core parameters selected for this more optimistic illustration and the corresponding figures for the previous conservative case are summarized in Table 5.1 (all factors are the same except capsule wall thickness).  Based on thermal and nuclear calculations, the parameters listed in Table 5.2 are found to be consistent with these specifications.

TABLE 5.1

Input Core Parameters

|  |  | Conservative Case | More Optimistic Case |
| --- | --- | --- | --- |
| Reactor power | [MWt] | 2500 | 2500 |
| $T_{inlet}$ | [°C] | 460 | 460 |
| $T_{max}$(interface) in average channel | [°C] | 750 | 750 |
| Capsule outside diameter | [cm] | 1.5 | 1.5 |
| Capsule wall | [cm] | 0.05 | 0.03 |
| Capsule fueled length | [cm] | 190 | 190 |
| Pins/subassembly[a] |  | 19 | 19 |
| Number of modules in reactor |  | 7 | 7 |

---

[a] A regular, rather than a corrugated, hexagonal subassembly can (see Ref. 2) is used in the present case.


TABLE 5.2

Inferred Core Parameters

|  |  | Conservative Case | More Optimistic Case |
| --- | --- | --- | --- |
| Core power | [MWt] | 1900 | 1650 |
| Core power fraction |  | 0.76 | 0.66 |
| Number of capsules |  | 3591 | 3059 |
| Number of subassemblies/module |  | 27 | 23 |
| Core sodium flow |  | $8.2 \cdot 10^3$ | $7.2 \cdot 10^3$ |
| $T_{inlet}$ | [°C] | 460 | 460 |
| $T_{outlet}$ | [°C] | 644 | 644 |
| Thermal stress (max) | [$10^3$ psi] | 8.3 | 5.1 |
| Core $\Delta P$ | [psi] | 10.3 | 10.5 |
| Fuel volume | [$10^3$ liter] | 1.09 | 0.98 |
| Nominal fuel density | [g Pu/cc fuel] | 3.7 | 3.8 |
| Loading (beginning-of-life) | [kg Pu] | 4000 | 3710 |
| Loading (equilibrium) | [kg Pu] | 3600 | 3340 |
| Breeding ratio |  | 1.37 | 1.65 |

As can be seen from the data of Table 5.2, the core power fraction is appreciably lower for the present case. This results from the more effective metal blanket. The harder neutron spectrum leads to a much higher $^{238}U$ fast fission contribution. The decreased core power, in turn, permits a corresponding decrease in the number of capsules. This is reflected in the decrease from 27 to 23 subassemblies per module. The total core sodium flow has been decreased correspondingly, so that the power-to-flow ratio is unchanged. The thermal data indicate that the more optimistic case is, in fact, conservative with regard to interface temperature and stress. Nuclear calculations show that the fuel density is not appreciably affected by these changes. The breeding ratio, however, is greatly improved.

The fabrication basis used to estimate fuel cycle costs for this revised case is given in Table 5.3. All factors not given in this table are taken as being equal to those used for the reference case (Table 3.2). A plutonium flow sheet is shown in Fig. 5. It will be noted that the use of a metallic blanket and the assumed use of nonaqueous reprocessing avoid the necessity of makeup feed conversion. The following discussion covers only those areas in which a specific and significant change in costs would be expected. All factors not discussed, such as the general process flow, procedures, and inspection, are assumed to be unchanged.

### 5.1.1  Capsule Manufacture

A simple capsule design is again assumed. In this case, a bottom cap and a machined transition piece are assumed to be welded to drawn tubing. Tantalum-5 w/o tungsten tubing, 1.5-cm diam x 0.03-cm wall, is procured as before at the price of $50/lb ($110/kg) for ingot plus $9/ft ($0.30/cm) for working and drawing to size.

TABLE 5.3

Specific Cost Bases

| | | Conservative Case | More Optimistic Case |
|---|---|---|---|
| Fuel | | | |
|   Plutonium content | [g/cc] | 3.7 | 3.8 |
|   Fuel composition | | | |
|     Plutonium | | 40.4 | 41.4 |
|     Cobalt | | 49.4 | 48.5 |
|     Cerium | | 10.2 | 10.1 |
| | | | |
| Capsule | | | |
|   Material | | Ta-5W | Ta-5W |
|   Fuel region | | | |
|     Length | [cm] | 190 | 210 |
|     Outside diameter | [cm] | 1.5 | 1.5 |
|     Wall thickness | [cm] | 0.05 | 0.03 |
|   Vent tube[a] or gas space | | | |
|     Length | [cm] | 190 | 240 |
|     Outside diameter | [cm] | 1.5 | 0.3 |
|     Wall thickness | [cm] | 0.05 | 0.03 |
| | | | |
| Number of fuel elements | | 3591 | 3059 |
|   Fuel content | [kg Pu] | 1.09 ea | 1.18 ea |
| | | | |
| Fuel volume | [liters] | $1.05 \cdot 10^3$ | $0.947 \cdot 10^3$ |

_____

[a] This small tube vents the volatile fission products into the cover gas.

BURNUP

LOSS

LOSS

980 kg

13.7 kg
(1/2 %)

19.4 kg
(1/2 %)

CORE   2730 kg   PYRO-CHEMICAL
REPROCESS   2716.3 kg   FABRICATION
3885 kg   FEED 1014 kg

154.2 kg   155 kg
(4%)

PYRO-CHEMICAL
REPROCESS

0.8 kg
(1/2 %)

LOSS

3710 kg
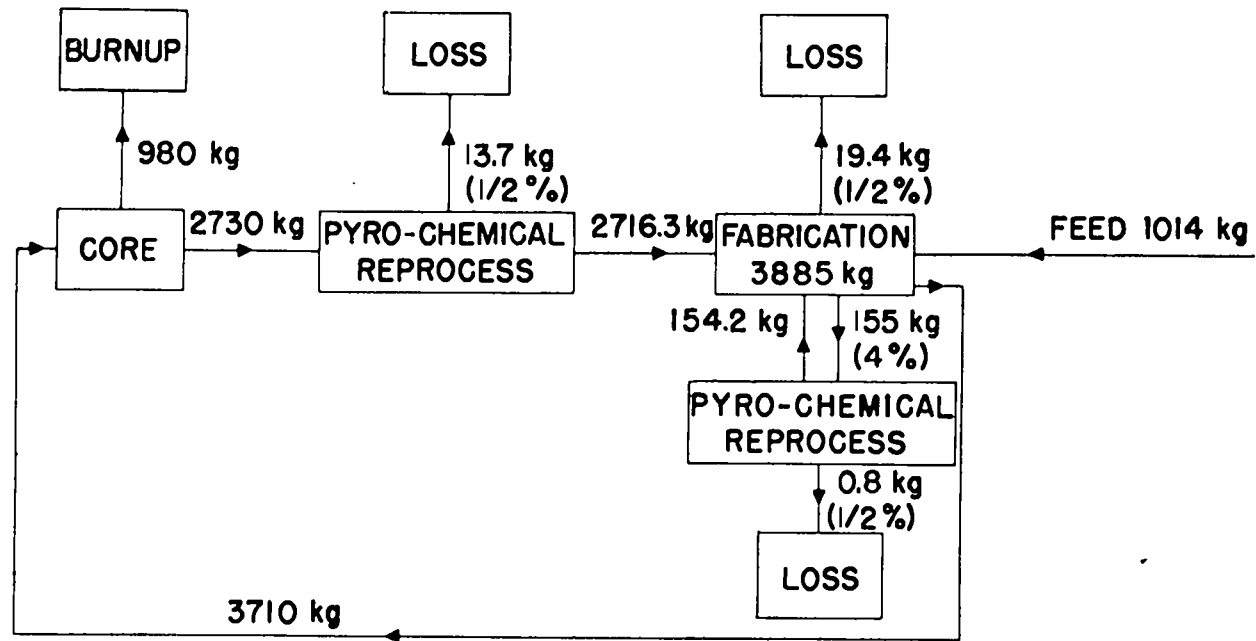
Fig. 5.   Flow Sheet for 1000-MWe Core Study

Fuel element tubing weight

$$= (16.6[g/cc])(\pi/4)(1.5^2 - 1.44^2[cm^2])(210[cm/capsule])$$

$$= 0.48[kg/capsule]$$

Fuel element tubing cost

$$= 0.48[kg/capsule] \cdot 110[\$/kg] + 210[cm/capsule] \cdot 0.3[cm^2]$$

$$= \$116/capsule$$

Vent tubing weight

$$= (16.6[g/cc])(\pi/4)(0.3^2 - 0.24^2[cm^2])(240[cm/capsule])$$

$$= 0.10[kg/capsule]$$

Vent tubing cost

$$= 0.10[kg/capsule] \cdot 10[\$/kg] + 240[cm/capsule] \cdot 0.3[\$/cm]$$

$$= \$83/capsule$$

Total cost of tubing

$$= \$200/capsule$$

Fabrication of the tubing into capsules is estimated to be similar to that used in Section 3. Thus, no significant change in this part of the fabrication cost ($32/capsule) is involved. The total nonfuel fabrication cost is then $230/capsule. This is equivalent to 0.09 $P_c$[mil/kWhe].

### 5.1.2  Fuel Fabrication, Capsule Loading, and Associated Costs

The cost per kilogram for fuel fabrication and capsule loading is not substantially changed. However, it can be assumed that a nonaqueous recovery of scrap is available, reducing the cost of recovery from $80/kg to ≈$7/kg. A corresponding reduction in fabrication losses from 1% to 0.5% may also be realistic, reducing the associated charges from $74/kg to ≈$37/kg. The feed conversion charge will not be incurred. The net effect of price changes is to reduce the fuel-dependent fabrication costs from $750/kg to $200/kg.

## 5.1.3 Other Charges

There is no change in the treatment used for working capital. A full pyrochemical processing cost may be assumed as ≈$175/kg residual plutonium plus ≈$38/kg for 0.5% losses, a total of $213/kg. The previous evaluation resulted in a total of $421/kg plutonium. A significant change in net plutonium charge results from the change in breeding ratio. The remaining core cost factors are also refigured, based on the data given in Tables 5.2 and 5.3. A summary comparison including the resulting effect of these factors on the fuel cycle costs is indicated in Table 5.4 (cf Table 3.3).

## 5.1.4 Summary Comparison

It is of some interest to identify the specific bases for the 0.4 mil difference in costs implied by the more optimistic bases. Clearly, the three significant differences are in fabrication, fuel recycle, and plutonium credit.

In fabrication the bulk of the difference comes from the reduction in the conversion charge in the makeup. This is associated with the metallic blanket form and the explicit assumption that the reprocessing scheme adopted for a metallic blanket will have as a product material which is, or which can be readily converted to, metal. The other differences contribute minor improvements to fabrication costs.

The reprocessing difference is identified with the increased yield assumed for the pyrochemical process, eliminating the need for aqueous reprocessing of skulls.

The third major effect is that associated with the change in the plutonium credit. This difference is associated with both the thin clad and the metallic blanket. The thin clad contributes an improvement of ≈0.1 in breeding ratio; the metallic blanket contributes 0.2 to 0.3 in breeding ratio, with the two not being strictly additive.

## TABLE 5.4

### Cost Comparison
[mil/kWhe]

| | Conservative Case | More Optimistic Case |
|---|---|---|
| Fabrication (including losses) | | |
|     Fuel-independent | 0.09 | 0.06 |
|     Fuel-dependent | 0.23 | 0.05 |
| | | |
| Capital | 0.01 | nil |
| Reprocessing[a] | 0.09 | 0.04 |
| Plutonium inventory[b] | 0.45 | 0.41 |
| Shipping | nil | nil |
|     Subtotal | 0.87 | 0.56 |
| | | |
| Radial blanket | 0.41 | 0.41 |
|     Subtotal | 1.28 | 0.97 |
| | | |
| Net plutonium charge | (0.25) | (0.39) |
|     Net Total | 1.03 | 0.58 |

---

[a] Including losses.
[b] At 10% inventory charge rate.

## 5.2 Alternative Geometries

A modular geometry has been assumed for this study, largely on the basis of convenience. Several alternative geometries are available which have certain advantages and disadvantages relative to the modular array.[11] From a nuclear point of view, there is little direct basis for selection among the various high-leakage core geometries. There are, however, specific features of each geometry that are of interest. For example, the moving fuel control scheme is likely to be more effective in an array of tall modules or in a tall annulus than in other geometries because it can be used to change effective core size, composition, and/or coupling. A flatter core, on the other hand, is less likely to be limited by coolant flow. In a pancake core, for which the effective blanket is that above and below the core, power shifts from core to blanket occur within a given coolant path.

If a metallic blanket is used, the incentive to utilize separate spectra in core and blanket is reduced. It thus becomes feasible to consider intermixed core and blanket elements, simulating an internal breeder. In addition to reducing the power shift, should this be of concern, a significantly improved $^{238}$U fast fission factor would be available. Some caution would be required to provide a simple fuel handling and management scheme.

## 5.3 Alternative Container Materials

A significant improvement in performance is available, should a suitable container be developed which has a lower neutron capture cross section than does tantalum. Such a change could be utilized in several ways. With no other change in design (assuming thermal performance to be satisfactory), the breeding ratio might be increased by about 0.25. Alternatively, a substantial decrease in fuel density, resulting in an increase in specific power, could be utilized to reduce the inventory charges. It is also reasonable to consider simulated internal breeding by intermixing blanket pins with the core, if a lower cross-section

62

container is available. The optimum compromise between fast fission factor gain and loss in $\eta$ of the fuel will depend on the detailed case being considered. It is estimated that any of these utilizations would be worth approximately 0.2 mil/kWhe in the fuel cycle cost.

## 5.4  Liquid Fuel Handling

With a liquid fuel, it may be feasible to use a plumbed system. While no detailed work has been done to compare such a system to the fixed fluid form used here, several general observations may be made. Assuming that containment is suitable for the life of the plant and that the fabrication cost of a plumbed system is of the same magnitude as for a capsule system, the nonfuel fabrication costs could be effectively eliminated. As was seen in Section 3, this would result in a fuel cycle cost saving of up to 0.09 mil/kWhe.

Fluid handling of the fuel might also allow an increase in the duty cycle of the plant. Among the fuel cycle cost factors, only the inventory charge would change. The incremental fuel cycle cost in going from 80% to 90% load factor, for example (using the figures of Table 3.5), is shown in Table 5.5. Data are also shown assuming a plant and operating cost of 2.5 mil/kWhe at 80% load factor. The saving in average power cost ($\approx$0.3 mil/kWhe) is in the same range as any other major improvement (such as an improvement in breeding ratio).

TABLE 5.5

Effect of Load Factor on Fuel Cycle and Power Costs

| | Units | Fuel Cycle Costs | | Power Costs | |
|---|---|---|---|---|---|
| Load factor | | 80% | 90% | 80% | 90% |
| Net cost, excluding inventory | [mil/kWhe] | 0.58 | 0.65 | 3.08 | 3.15 |
| Inventory charge | [mil/kWhe] | 0.40 | 0.40 | 0.40 | 0.40 |
| Cost | [mil/kWhe] | 0.98 | 1.05 | 3.48 | 3.55 |
| Power | [relative units] | 1.0 | 1.125 | 1.0 | 1.125 |
| Average cost/unit power | [mil/kWhe] | 0.98 | 0.93 | 3.48 | 3.16 |
| Base cost for first 80% | [mil/kWhe] | 0.98 | 0.98 | 3.48 | 3.48 |
| Incremental charge | [mil/kWhe] | | 0.07 | | 0.07 |
| Incremental power | [relative units] | | 0.125 | | 0.125 |
| Incremental cost | [mil/kWhe] | | 0.56 | | 0.56 |

APPENDIX A

BREEDING FACTORS

For reactors in which the axial leakage is a relatively small compo-
nent of the neutron balance, it is possible to use a buckling-corrected
one-dimensional representation for survey work. While this is quite
adequate for most neutronic properties, the breeding ratio is sensitive
to relatively small terms in the neutron balance. Thus, it is appropriate
to make some allowance for axial leakage in calculating breeding ratios.
The following procedure is used for this cycle cost study. Two factors
are defined: a radial breeding factor and a radial plus axial breeding
factor. Although these are estimates of a breeding ratio, they are
referred to as breeding factors rather than breeding ratios to minimize
misunderstanding.

## A.1  Radial Breeding Factors

The radial breeding factor BF(R) ignores the axial blanket contri-
bution to net production of fissile material and is defined by

$$
BF(R) = \frac{\displaystyle\sum_{k=1}^{k_{max}} \sum_{g=1}^{g_{max}} \Sigma_{c,g,k}^{28+40} \phi_g}{\displaystyle\sum_{k=1}^{k_{max}} \sum_{g=1}^{g_{max}} \Sigma_{a,g,k}^{49+25} \phi_g} , \qquad (A.1)
$$

where

    k denotes the core and radial blanket regions,
    g denotes the group,
    c denotes capture,
    a denotes absorption, and
    (28,40)(49,25) are the fertile and fissile isotopes, respectively.

Equation (A.1) amounts to total captures per unit time in fertile material divided by total absorption per unit time in fissile material, in both core and radial blanket. This factor can be obtained directly from one-dimensional calculations.

## A.2  Axial Correction

In order to approximate the contribution of the axial blankets to the breeding ratio, the following procedure was devised to estimate axial blanket absorption in fissile material and capture in fertile material.  The total axial neutron leakage is described by

$$L_{ax} = L_1 + L_2 + L_4 + L_4, \tag{A.2}$$

where $L_4$ and $L_1$ are, respectively, the leakage out of the top and bottom of the core, and $L_3$ and $L_2$ are, respectively, the leakage out of the top and bottom of the remaining regions (radial blanket and reflector).  The following additional parameters are defined:

$A^i \equiv$ absorption in all materials of region i,

$S^i \equiv$ source in region i,

$A^i_{49+25} \equiv$ absorption in 49 and 25 in region i,

$C^i_{49+28} \equiv$ capture in 40 and 28 in region i,

where the superscript i refers to core, radial blanket (RB), reflector, or axial blanket (AB).  Except for the axial blanket, these quantities can be obtained from the one-dimensional calculation.  Further, let A be the total absorption plus axial leakage.  The axial leakage, $L_{ax}$, included in A is the fictitious buckling absorption and may be expressed as

$$L_{ax} = A - (A^{core} + A^{RB} + A^{ref}). \tag{A.3}$$

Now, let $L_{CB}$ be the net leakage from core to radial blanket.  This term is available from the one-dimensional calculation.  The total axial core

66

leakage may be expressed by

$$L_1 + L_4 = S^{core} - L_{CB} - A^{core}. \tag{A.4}$$

It is assumed that the core leakage above and below are equal, i.e.,

$$L_1 = L_4.$$

The total axial blanket leakage is expressed by

$$L_2 + L_3 = L_{ax} - (L_1 + L_4). \tag{A.5}$$

Now, let us define a parameter $\alpha_i$ by

$$\alpha_i = \frac{S^i}{A^i}, \tag{A.6}$$

where $i = RB, AB$. It is assumed that $\alpha$ in each blanket region is the same, i.e.,

$$\alpha_{RB} = \alpha_{AB} = \alpha. \tag{A.7}$$

Assume further that to a first-order approximation, absorptions in either blanket are given by

$$A^i = L^i + \int_{Reg\ i} dV \sum_g \phi_g (\nu\Sigma_f)_g \tag{A.8}$$

or, equivalently, by

$$A^i = L^i + S_i. \tag{A.9}$$

Note that this assumes no leakage beyond the blanket. For relatively thin blankets, this is inappropriate. In fact, for the cases considered, this may result in a 5 to 10% overestimate of the breeding ratio. As with other factors, however, no error in the comparison of concepts should be introduced.

From the definition of $\alpha$ (Eq. A.6), we may write

$$\alpha_i = \frac{(A^i - L^i)}{A^i}$$

$$A^i = \frac{L^i}{(1 - \alpha_i)} \; . \tag{A.10}$$

The value of $\alpha_{RB}$ can be obtained from the edit of the one-dimensional problem and with Eqs. A.7 and A.10 can be used to find $A^{AB}$.

Since the top leakage from the liquid plutonium cores is to the gas space rather than to the blanket material, it is convenient to consider each axial blanket subregion separately. Let $A_j^{AB}$, defined by

$$A_j^{AB} = \frac{L_i^{AB}}{1 - \alpha} \; , \tag{A.11}$$

be the absorptions in each axial blanket subregion j. Then assume that because the radial and axial blanket have similar compositions,

$$A_{j,49+25}^{AB} = \left( \frac{A_{49+25}^{RB}}{A^{RB}} \right) A_j^{AB}$$

$$C_{j,40+28}^{AB} = \left( \frac{C_{40+25}^{RB}}{A^{RB}} \right) A_j^{AB} \; . \tag{A.12}$$

Then, the total absorption in fissile material is

$$A_{49+25}^{T} = A_{49+25}^{core} + A_{49+25}^{RB} + \sum_j A_{j,49+25}^{AB} \; , \tag{A.13}$$

and the contribution from each region or subregion r to the breeding factor is

$$BF^r = \frac{C_{40+28}^r}{A_{49+25}^T} \; , \qquad r = core, RB, AB(1), AB(2), AB(3), AB(4). \tag{A.14}$$

The radial plus axial breeding factor is then given by

$$BF(R + A) = \sum_r BF^r \qquad (A.15)$$

where it should be noted that the axial blanket subregion above the core contributes nothing in the case of the liquid plutonium cores.

A simple FORTRAN code (LABRR) was devised for computing one-dimensional (radial) breeding factors according to Eq. (A.1) and approximate two-dimensional (radial plus axial) breeding factors according to Eq. (A.15). The code uses output from the DTF code as input, and calculations are restricted to the type of module considered in this report.

# APPENDIX B

## BURNUP UNITS

Various units are used to express the amount of energy extracted
from a given amount of fuel. The preferred unit depends on its utility
relative to a particular discussion or on its relationship to fuel-life
limiting mechanisms. Traditionally, units of

> fission/cc (f/cc)
> MWd/T
> % burnup

have been used. The volumetric unit (f/cc) is frequently preferred
because it is a measure of volumetric generation of volatile fission
products whose retention is thought to be related to fuel swelling
phenomena, a limiting factor on burnup capability. This unit has several
disadvantages, one being that the numerical magnitude (of the order of
$10^{21}$) is inconvenient and not easily visualized. Further, the relation-
ship of this unit to parameters of economic or resource interest is not
readily apparent.

The other common units (MWd/T and % burnup) are not thought to be
related to materials capability. The MWd/T unit is ambiguous as to
whether the denominator is a long, short, or metric ton -- and as to
whether the mass is a ton of the fuel material or of heavy atoms. A
unit of MWd/kg is more convenient but does not avoid all of the above
problems. Similarly, with % burnup, it is not clear whether the burnup
is in percentage of total atoms, heavy atoms, or fissile atoms -- or
perhaps on a weight-percentage basis.

The unit "g fissioned/cc fuel" avoids some of the obvious difficulties
referred to above. It is a volumetric unit and thus is presumably related
to burnup capability. In addition, the magnitude is convenient, in that

common burnup goals are of the order of 1 gf/cc.  This is related to %
burnup by means of a density, which is usually available.  The only
ambiguity lies in the fuel density (or volume) used -- whether initial
or current value and whether including or excluding bond volume.  In
this study, bond volume is not considered as part of the fuel volume,
and initial fuel density is used.

Table B.1 lists conversion factors for some of the more commonly
used burnup units.

TABLE B.1

Burnup Units Equivalent to 1 gf/cc[a]

| | Oxides[b] | Carbides[c] | Solid Metals[d] | Liquid Metals[e] |
|---|---|---|---|---|
| gf/cc | 1.0 | 1.0 | 1.0 | 1.0 |
| gf/cc smeared[f] | 0.90 | 0.95 | 0.80 | 0.95 |
| % BU of HA | 12.17 | 9.09 | 6.54 | 25.0 |
| MWd/metric ton HA | 114,100 | 85,200 | 61,200 | 234,200 |
| MWd/long ton HA | 115,900 | 86,600 | 62,200 | 238,000 |
| MWd/short ton HA | 103,500 | 77,300 | 55,500 | 212,500 |
| MWd/metric ton fuel | 100,600 | 81,100 | 55,100 | 100,500 |
| MWd/long ton fuel | 102,200 | 83,000 | 56,000 | 102,100 |
| MWd/short ton fuel | 91,300 | 73,600 | 50,000 | 91,200 |
| f/cc | $25.3 \cdot 10^{20}$ | $25.3 \cdot 10^{20}$ | $25.3 \cdot 10^{20}$ | $25.3 \cdot 10^{20}$ |
| f/cc smeared | $22.8 \cdot 10^{20}$ | $24.0 \cdot 10^{20}$ | $20.2 \cdot 10^{20}$ | $24.0 \cdot 10^{20}$ |

------

[a] Based on 199 MeV/fission = $3.2 \cdot 10^{-17}$ MW-sec/fission.
$\qquad$ = $8.1 \cdot 10^4$ MW-sec/gf $\approx$ 0.937 MWd/gf.

[b] Oxides are taken to have a density of 9.316 g/cc (85% of theoretical),
$\qquad$ smeared density of 8.384 g/cc (90 v/o fuel; 10 v/o bond)

[c] Carbides are taken to have a density of 11.56 g/cc (85% of theoretical)
$\qquad$ smeared density of 10.98 g/cc (95 v/o fuel; 5 v/o bond)

[d] Solid metals are taken to have a density of 17 g/cc (90 w/o heavy atoms)
$\qquad$ smeared density of 13.6 g/cc (80 v/o fuel; 20 v/o bond)

[e] Liquid metals are taken to have a density of 9.32 (4 g Pu/cc fuel)
$\qquad$ smeared density of 8.85 g/cc (95 v/o fuel; 5 v/o bubbles)

[f] Smeared density is the ratio of fuel mass to total internal volume of the fuel region of the fuel element, including bond volume. The smeared densities used are illustrative.

APPENDIX C


TEMPERATURE, PRESSURE DROP, AND VELOCITY LIMITS


The thermal-hydraulic factors limiting core design are:
1. capsule thermal stress
2. capsule hoop stress
3. core sodium velocity
4. core sodium pressure drop
5. fuel-capsule interface temperature.

The capsule thermal stress limit is discussed in Appendix D, and the capsule hoop stress limit is discussed in Appendix E. The other limits may be expressed in such a way as to estimate the minimum number of capsules needed to satisfy the limits as a function of pitch-to-diameter ratio. A fixed capsule diameter, fuel height, and core power are assumed. The equations herein are intended as a guide in estimating suitable parameter ranges. A more precise analysis, such as is available with the computer code HTHX,[22] should be used to verify the results for specific cases.


## C.1 Core Sodium Velocity

Core sodium velocity may be a limit on core design for reasons of pressure drop, corrosion, or vibration. The pressure drop will be considered later in this appendix. An arbitrary maximum velocity limit is normally considered. The sodium velocity in a triangular lattice of fuel elements is given by

$$v = \frac{W(M/A)_R}{\rho_N \, N(0.866 \, P^2 - \frac{\pi}{4} D^2)} \tag{C.1}$$

where

     $W$ = sodium mass flow rate

     $\rho_N$ = sodium density

     $N$ = number of capsules

     $P$ = capsule centerline-to-centerline spacing

     $D$ = capsule outer diameter

     $v$ = sodium velocity

$(M/A)_R$ = radial maximum-to-average power ratio
         (perfect orificing is assumed).

The minimum allowable number of fuel elements is that which corresponds to the maximum permissible coolant velocity $v_{max}$. From Eq. (C.1), this is

$$N_{min}^{v} = \frac{W(M/A)_R}{\rho_N\, v_{max}\left(0.866\, P^2 - \frac{\pi}{4}\, D^2\right)} \tag{C.2}$$

## C.2  Core Coolant Pressure Drop

The pressure drop due to coolant flow past the fuel elements (no structure or spacers) is given by

$$\Delta p = \frac{4fh(1 + \alpha)}{D_{ep}}\, \rho_N\, \frac{v^2}{2g} \tag{C.3}$$

where

     $\Delta p$ = core pressure drop

     $h$ = fuel length

     $g$ = gravitational constant

     $\alpha$ = gas-to-fuel volume ratio

     $D_{ep}$ = equivalent diameter for pressure drop

     $f$ = friction factor.

The friction factor, $f$, is given by

$$f = \begin{cases} 16/Re & \text{for } Re < 2500 \\ 0.0014 + 0.125\, Re^{-0.32} & \text{for } Re \geq 2500 \end{cases} \tag{C.4}$$

For most cases to be considered, the Reynolds number (Re) >> 2500, and an assumption of constant friction factor, $f = f_0$, is fairly accurate. The equivalent diameter for pressure drop should include the effect of drag on subassembly can walls and fuel element separators (wire wrapping or egg crates) and entrance and exit losses. To simplify the calculations, neglect these and assume that the equivalent diameter for pressure drop is the same as that for heat transfer, namely,

$$D_{ep} = D_{eH} = D_e = \frac{4 \cdot \text{cross sectional area}}{\text{wetted perimeter}}$$

$$= \frac{4(0.866 \ P^2 - \frac{\pi}{4} D^2)}{\pi D}$$

$$= D[1.103(P/D)^2 - 1] \qquad \qquad (C.5)$$

The major unknown in the pressure drop calculation is the effect of structure on $f$ and on $D_{ep}$. It has been estimated that such structure could increase the pressure drop by a factor of 2 to 4 over the smooth tube pressure drop. The core pressure drop, if the effect of structure is a factor of 3, is

$$\Delta p = \frac{0.02918 \ h(1 + \alpha) \ W^2 (M/A)_R^2}{\rho_N \ g \ D_e^3 \ N^2 \ D^2} \qquad \qquad (C.6)$$

for $f_0 = 3 \cdot 10^{-3}$ (corresponding to Re $= 5.9 \cdot 10^5$). Substituting Eq. (C.5) into Eq. (C.6) and rearranging yields

$$N_{min}^P = \frac{0.1709 \ W(M/A)_R}{D^{2.5}[1.103(P/D)^2 - 1]^{1.5}} \left[ \frac{h(1 + \alpha)}{\rho_N \ g \ \Delta p_{max}} \right]^{0.5} \qquad (C.7)$$

as the minimum allowable number of capsules to satisfy an allowable core pressure drop, $\Delta p_{max}$.

## C.3  Fuel-Capsule Interface Temperature

The fuel-capsule interface temperature is given by

$$T_W(Z) = T_{in} + \Delta T_M(Z) + \Delta T_F(Z) + \Delta T_W(Z) \qquad (C.8)$$

where

$T_{in}$ = core inlet sodium mixed mean temperature

$$\Delta T_M(Z) = \frac{1}{C_p W} \int_0^Z Q'(Z) \, dZ = \text{mixed mean temperature rise} \qquad (C.9)$$

$$\Delta T_W(Z) = \frac{Q'(Z)(M/A)_R}{2\pi \, k_W N} \ln\left(\frac{D}{D-2t}\right) = \text{wall temperature drop} \qquad (C.10)$$

$$\Delta T_F(Z) = \frac{Q'(Z)(M/A)_R}{\pi D H N} = \text{coolant film drop} \qquad (C.11)$$

where

$Z$ = core height

$H$ = film heat transfer coefficient

$k_W$ = capsule wall thermal conductivity

$t$ = capsule wall thickness

$C_p$ = coolant specific heat

$Q'(Z)$ = total core power per unit height of fuel at height Z.

The heat transfer coefficient, H, is given by

$$H = \frac{k_N Nu}{D_{eH}} \qquad (C.12)$$

where

$k_N$ = sodium thermal conductivity

$Nu$ = Nusselt number.

The equivalent diameter for heat transfer, $D_{eH}$, is given by Eq. (C.5). Use of Dwyer's correlation,[33]

$$Nu = 0.93 + 10.81(P/D) - 2.01(P/D)^2 + 0.0252(P/D)^{0.273}(\bar{\psi} \, Re \, Pr)^{0.8},$$

(C.13)

where

$\bar{\psi}$ = ratio of heat transfer eddy diffusivity to momentum transfer eddy diffusivity

$Re$ = Reynolds number

$Pr$ = Prandtl number,

makes a closed solution for N impossible. Numerical results, such as the example given below, indicate that the Nusselt number does not vary a great deal between cases of interest (i.e., cases which avoid extremes of D, P/D, and N). Hence, to facilitate the calculation, it will be assumed that the Nusselt number is constant over the range of interest, $N = Nu_0$. Putting this and Eqs. (C.9), (C.10), (C.11), (C.12), and (C.5) into (C.8):

$$T_W(Z) - T_{in} = \frac{1}{C_p W} \int_0^Z Q'(Z) \, dZ + \frac{Q'(Z)(M/A)_R [1.103(P/D)^2 - 1]}{\pi N \, k_N \, Nu_0}$$

$$+ \frac{Q'(Z)(M/A)_R \ln\left(\frac{D}{D - 2t}\right)}{2\pi \, k_W \, N},$$

(C.14)

the solution of Eq. (C.14) for N is

$$N_{min}^H = \left\{ \frac{\frac{[1.103(P/D)^2 - 1]}{k_N \, Nu_0} + \frac{1}{2k_W} \ln\left(\frac{D}{D - 2t}\right)}{T_W^{max}(Z) - T_{in} - \frac{1}{C_p W} \int_0^Z Q'(Z) \, dZ} \right\} \frac{Q'(Z)(M/A)_R}{\pi},$$

(C.15)

which is the minimum allowable number of capsules that satisfies the interface temperature limit. HTHX calculations[22] have generally shown the maximum interface temperature to occur at a height of 0.8 to 0.9 times

the fuel length. A value of 0.85 will be used. It will further be assumed that the power distribution has the same shape as the MPBE,[2] so that

$$(M/A)_R = 1.3$$

$$Q'(\text{at } Z = 0.85 \text{ h}) = 0.857 \, P_c/h \tag{C.16}$$

$$\int_0^{0.85L} Q'(Z)dZ = 0.931 \, P_c. \tag{C.17}$$

Substituting these into Eq. (C.15) gives

$$N_{min}^H = \left\{ \frac{\frac{1}{k_N \, Nu_0}[1.103(P/D)^2 - 1] + \frac{1}{2k_W} \ln\left(\frac{D}{D - 2t}\right)}{\left[T_W^{max}(\text{at } 0.85 \text{ h}) - T_{in}\right] - \frac{0.931 \, P_c}{C_p W}} \right\} \left(\frac{0.355 \, P_c}{h}\right). \tag{C.18}$$

## C.4  Numerical Example

Certain physical constants as used in this study are given in Table C.1.

### TABLE C.1

### Selected Physical Constants

| | | |
|---|---|---|
| Sodium thermal conductivity, $k_N$ | [W/cm °C] | 0.637 |
| Container thermal conductivity, $k_W$ | [W/cm °C] | 0.755 |
| Sodium specific heat, $C_p$ | [W-sec/g °C] | 1.27 |
| Sodium density, $\rho_N$ | [g/cc] | 0.817 |
| Gravitational constant, g | [cm/sec$^2$] | 980 |

The particular case is described by the factors given in Table C.2.

TABLE C.2

Specific Case Considered

| | | |
|---|---|---|
| Nominal flow, W | [kg/sec] | $12.2 \cdot 10^3$ |
| (M/A) radial | | $1.3^{(a)}$ |
| Maximum sodium velocity, $v_{max}$ | [cm/sec] | $1.22 \cdot 10^3$ |
| Gas-to-fuel volume, $\alpha$ | | 1.0 |
| Maximum pressure drop, $\Delta p_{max}$ | [kg/cm$^2$] | 4.22 |
| Fuel length, h | [cm] | 190 |
| Wall thickness, t | [cm] | 0.05 |
| Power level, $P_c$ | [MW] | 1900 |
| Capsule diameter, D | [cm] | 1.5 |
| $T_W^{max}$ (at 0.85 h) | [°C] | 750 |
| $T_{in}$ | [°C] | 460 |

(a) See Ref. 2.

The gas space length ($\alpha = 1.0$) is based on the allowable pressure rise, as described in Appendix E. This factor does not significantly affect the nuclear or thermal properties of the core but will affect costs somewhat. As shown in Appendix E, an $\alpha$ of 0.9 is adequate, but some margin is desirable.

With these values, Eq. (C.2) becomes

$$N^V_{min} = \frac{9000}{1.102(P/D)^2 - 1} ,$$

Eq. (C.7) becomes

$$N^P_{min} = \frac{10400}{[1.103(P/D)^2 - 1]^{1.5}} ,$$

and, for $Nu_0 = 25$, Eq. (C.18) yields

$$N_{min}^H = 1170[1.103(P/D)^2 - 1] + 850.$$

Figure 6 is a plot of the values of $N_{min}$ versus P/D for various flows relative to $12.2 \cdot 10^3$ kg/sec. It will be noted that, for the case shown, temperature and $\Delta p$ are the most likely limits. Had this case utilized a shorter core, a greater range would exist in which velocity would be limiting.
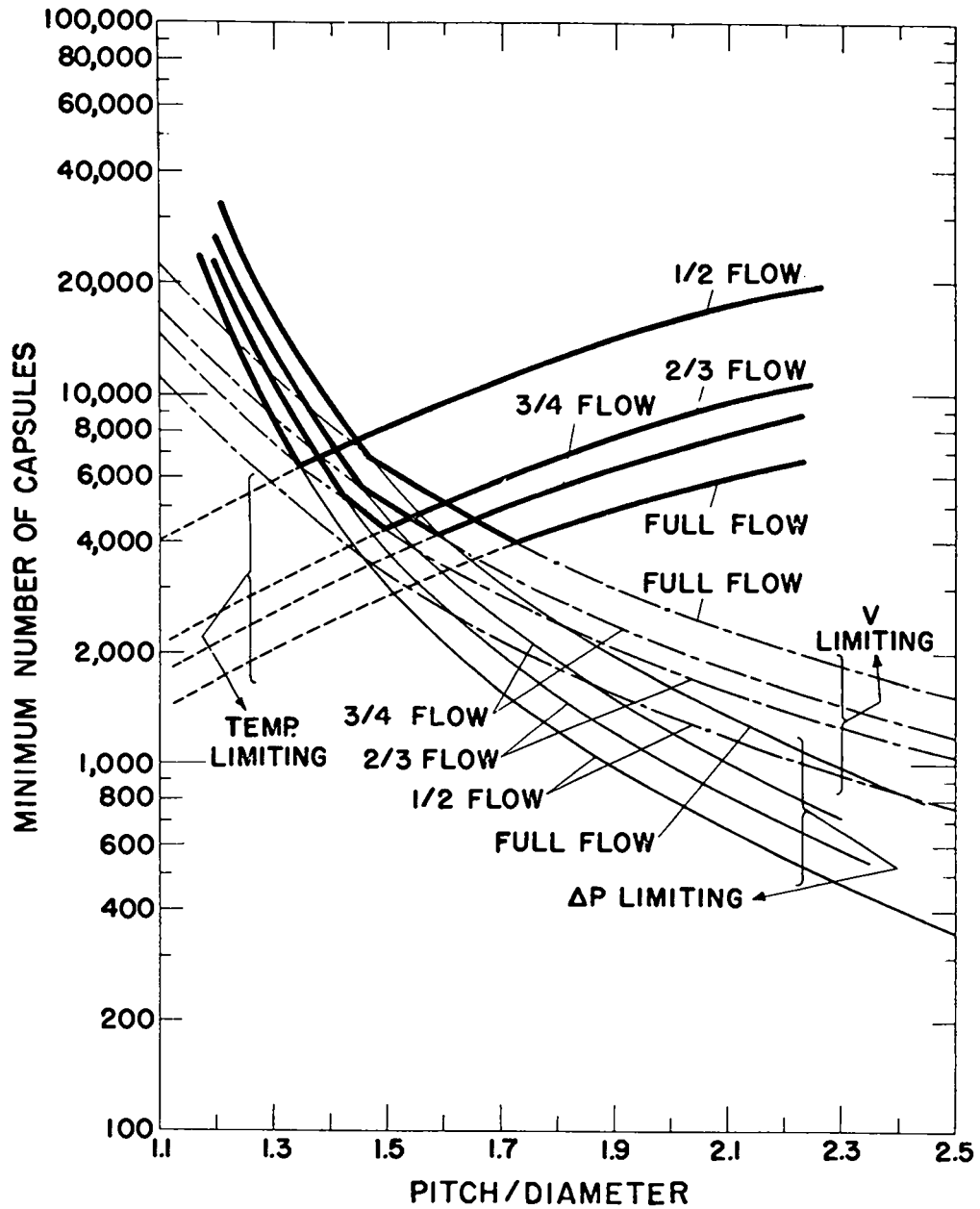
Fig. 6. Minimum Number of Fuel Capsules Consistent with Various
Limiting Criteria

## APPENDIX D

## THERMAL STRESS LIMITS

The maximum tensile thermal stress occurs at the exterior wall of the capsule and is given by

$$S_t = \frac{E \, A_t \, \Delta T_W^{max}}{2(1 - \nu) \ln \left(\frac{D}{D - 2t}\right)} \left[1 - \frac{2(D - 2t)^2}{D^2 - (D - 2t)^2} \ln \left(\frac{D}{D - 2t}\right)\right] \qquad (D.1)$$

where

$E$ = elastic modulus

$A_t$ = capsule wall coefficient of thermal expansion

$\Delta T_W^{max}$ = maximum radial wall temperature drop

$\nu$ = Poisson's ratio

$D$ = capsule outer diameter

$t$ = capsule wall thickness.

The maximum radial wall temperature drop is

$$\Delta T_W^{max} = \frac{P_c (M/A)}{2\pi \, k_W \, N \, L} \ln \left(\frac{D}{D - 2t}\right) \qquad (D.2)$$

where

$P_c$ = total core power

$(M/A)$ = maximum-to-average power ratio

$k_W$ = capsule wall thermal conductivity

$N$ = number of capsules

$h$ = core height.

Putting Eq. (D.2) into Eq. (D.1) yields

$$S_t = \frac{E \, A_t \, (M/A) \, P_c}{4\pi(1 - \nu)h \, k_W N} \left[ 1 - \frac{2(D - 2t)^2}{D^2 - (D - 2t)^2} \ln\left(\frac{D}{D - 2t}\right)\right]$$ (D.3)

Vented capsules at all times, and sealed capsules at the beginning of core life, are normally required to satisfy the condition

$$S_t \leq 2 \, S_y^0 \, ,$$ (D.4)

where $S_y^0$ is the capsule yield strength at the beginning of core life. As core burnup proceeds, it is normally required that vented capsules satisfy the less stringent (and therefore unnecessary) condition

$$S_t \leq 2 \, S_y \, ,$$ (D.5)

where $S_y$ is the capsule yield strength increased by tungsten burn-in and fast neutron bombardment, while sealed capsules must satisfy

$$S_t + S_H \leq 2 \, S_y \, ,$$ (D.6)

where $S_H$ is the hoop stress due to internal pressure. Since $S_H$ is a function of burnup and gas-to-fuel volume ratio in the capsule, and $S_t$ is not dependent on these parameters, it is a desirable simplification to treat $S_H$ and $S_t$ separately. A conservative way to do this is to consider the hoop stress at its limiting value

$$S_H = \frac{2}{3} \, S_y$$ (D.7)

and to ignore the increase in capsule yield strength due to irradiation. This gives

$$S_t \leq \frac{4}{3} \, S_y^0$$ (D.8)

as the applicable limit on thermal stress in a sealed capsule, in place of Eq. (D.6). If these conservative simplifications limit core design

more stringently than do other limits such as temperature, coolant velocity, or coolant pressure drop, then Eq. (D.6) should be used.* Substituting Eq. (D.8) into Eq. (D.3) and solving for the number of capsules gives

$$N_{min} = \frac{3(M/A) \, E \, A_t \, P_c}{16\pi(1 - \nu)h \, k_W \, S_y^0} \left[ 1 - \frac{2(D - 2t)^2}{D^2 - (D - 2t)^2} \ln\left(\frac{D}{D - 2t}\right) \right] \qquad (D.9)$$

as the minimum number of capsules which will satisfy the thermal stress limit Eq. (D.8) for sealed capsules. For vented capsules, the constant 3/16 is replaced by 1/8 .

As a numerical example, the parameters used for this study are given in Table D.1.

TABLE D.1

Specific Case Considered

| | | |
|---|---|---|
| Elastic modulus, $E$ | [kg/cm$^2$] | $1.7 \cdot 10^6$ |
| Yield strength, $S_y^0$ | [kg/cm$^2$] | $2.39 \cdot 10^3$ |
| Coefficient of thermal expansion, $A_t$ | [°C$^{-1}$] | $6.8 \cdot 10^{-6}$ |
| Power level, $P_c$ | [MWt] | 1900 |
| Fuel length, $h$ | [cm] | 190 |
| Conductivity, wall, $k_W$ | [W/cm °C] | 0.755 |
| Wall thickness, $t$ | [cm] | 0.05 |
| Poisson's ratio, $\nu$ | | 0.3 |
| Maximum-to-average power ratio, $(M/A)$ | | 1.48 |

Substituting the values given in Table D.1 into Eq. (D.9) gives

$$N_{min} = 8073 \left[ 1 - \frac{2(D - 2t)}{D^2 - (D - 2t)^2} \ln\left(\frac{D}{D - 2t}\right) \right] \qquad (D.10)$$

for sealed capsules. For vented capsules, the constant 8073 is replaced by 5382. These functions are plotted in Fig. 7.

---

*Thermal stress does not limit the core designs considered in this study. Therefore, the use of Eq. (D.8) is acceptable.
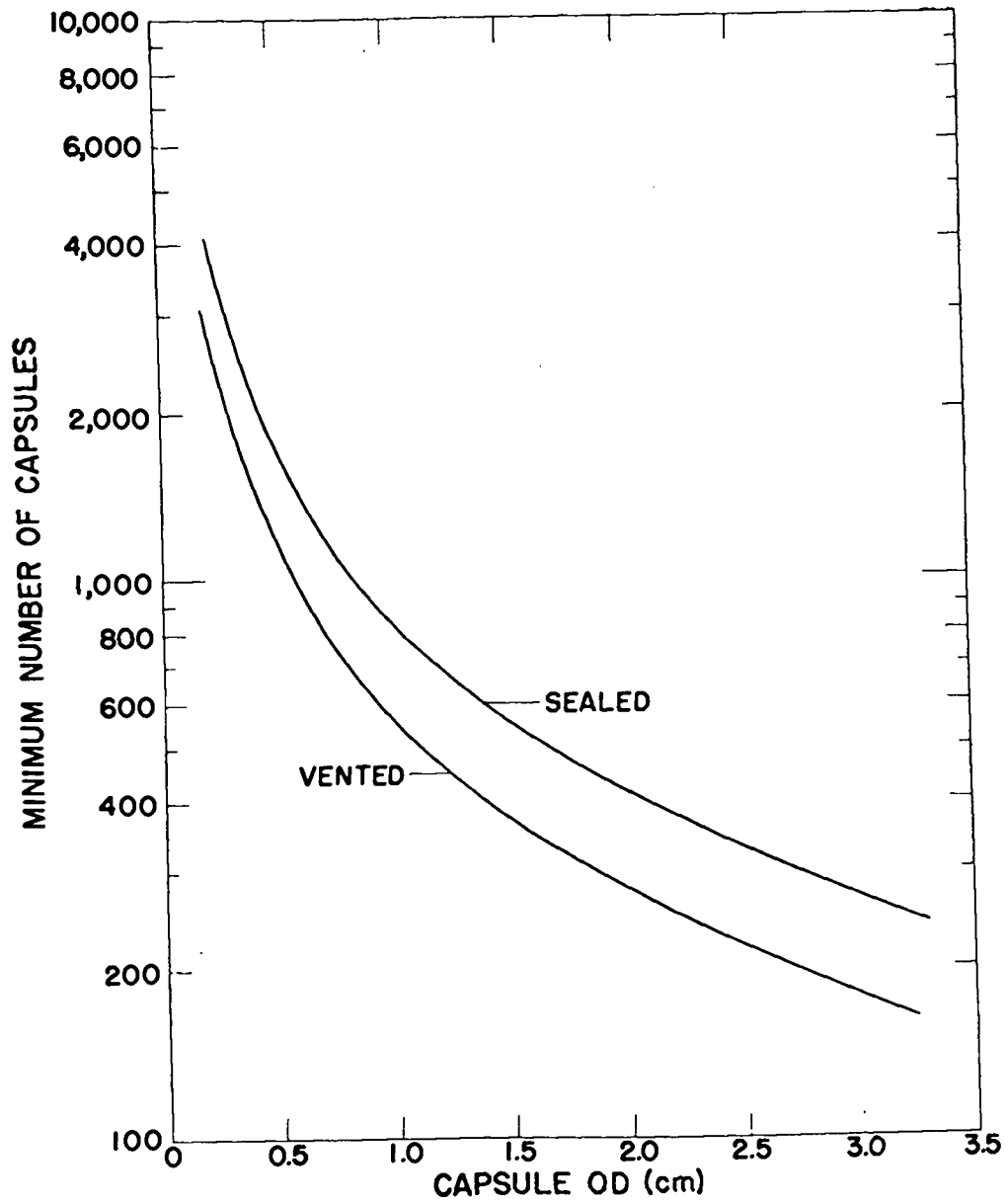
Fig. 7. Minimum Number of Capsules Required to Meet Thermal
Stress Limits

## APPENDIX E

## HOOP STRESS LIMITS

The hoop stress in the inner fiber of a capsule is given by

$$S_H = \frac{D^2 + (D - 2t)^2}{D^2 - (D - 2t)^2} \, p, \qquad \text{(E.1)}$$

where

D = capsule outer diameter,

t = wall thickness of capsule,

p = capsule internal pressure.

Equation (E.1) assumes that the external pressure on the capsule is zero. The hoop stress is normally required to satisfy the relation

$$S_H \leq \frac{2}{3} S_y, \qquad \text{(E.2)}$$

where $S_y$ = yield strength of capsule material [see Eq. (D.7)]. Since very little tungsten will be produced by neutron absorption at the top of the gas space, the value of $S_y$ at the beginning of core life should be used. Combining Eqs. (E.1) and (E.2) yields

$$p \leq \frac{2}{3} S_y \left[ \frac{D^2 - (D - 2t)^2}{D^2 + (D - 2t)^2} \right] \qquad \text{(E.3)}$$

From the value of p given by Eq. (E.3), the Beattie-Bridgeman relation can be used to find the minimum allowable molar volume, $V_m^{min}$. The molar volume is defined as

$$V_m = \frac{\text{gas volume}}{\text{moles of He + Kr + Xe}} \, . \qquad \text{(E.4)}$$

The number of moles of krypton and xenon combined is given by

$$V_F[cm^3] \cdot BU\left[\frac{g\ Pu\ fissioned}{cc\ fuel}\right] \cdot \frac{1}{239}\left[\frac{g\ atom\ Pu}{g\ Pu}\right] \cdot N_0\left[\frac{atoms\ Pu}{g\ atom\ Pu}\right]$$

$$\cdot\ 0.27\left[\frac{gas\ atoms}{Pu\ atoms\ fissioned}\right] \cdot \frac{1}{N_0}\left[\frac{mole\ gas}{gas\ atoms}\right]$$

$$=\ 0.00113 \cdot V_F \cdot BU[cc],$$

where

$N_0$ = Avogardo's number

$V_F$ = fuel volume

BU = burnup [gf/cc]

In addition, there is an initial filling of gas of approximately $3.0 \cdot 10^{-5}\ V_g$ moles of helium, where $V_g$ is the gas volume [cc]. A cumulative yield of stable isotopes of xenon and krypton of 27 per hundred fissions is used.[34] The molar volume [liters/mole] is then given by

$$V_m\ =\ \frac{V_g}{0.00113\ V_F \cdot BU + 3.0 \cdot 10^{-5}\ V_g}\left[\frac{cc}{mole}\right] . \tag{E.5}$$

Thus, the minimum allowable gas-to-fuel volume ratio is given by

$$\alpha_{min}\ =\ \left(\frac{V_g}{V_F}\right)_{min}\ =\ \frac{0.00113 \cdot BU}{(1/V_m^{min}) - 3.0 \cdot 10^{-5}} . \tag{E.6}$$

The Beattie-Bridgeman relation may be expressed (see, for example, Ref. 35) as

$$V_m\ =\ \frac{RT}{p} + \frac{\beta}{RT} + \frac{\gamma \cdot p}{(RT)^2} + \frac{\delta \cdot p^2}{(RT)^3} , \tag{E.7}$$

87

where

T is the temperature [°K]

R is the gas constant

$\beta$, $\gamma$, $\delta$ are constants characteristic of the gas considered.

For low pressures, it is reasonable to use a weighted average of Beattie-Bridgeman coefficients for xenon and krypton (This is not strictly correct but is adequate for the present application. Standard values for the constants of the gases[36] are used.) For the present case, a weighting of 24 parts xenon to 1 part krypton is used. With T = 700°C (973°K), the above terms become (R = 82.1 cc atm/°K mole)

$$\beta = 1.3149 \cdot 10^6$$

$$\gamma = 0.1490 \cdot 10^9$$

$$\delta = 0.0$$

$$RT = 79,880.$$

Thus, for this case,

$$V_m = \frac{79,880}{p} + 16.5 + 2.335 \cdot 10^{-2} \, p \, [cm^3/mole] \qquad (E.8)$$

for p in atmospheres.

Evaluating $\alpha$ as a function of capsule diameter from Eq. (E.6), and utilizing Eq. (E.8) gives the results plotted in Fig. 8. A yield strength of 34,000 psi and a wall thickness of 0.05 cm are assumed, and BU is taken to be 1.0 gf/cc.
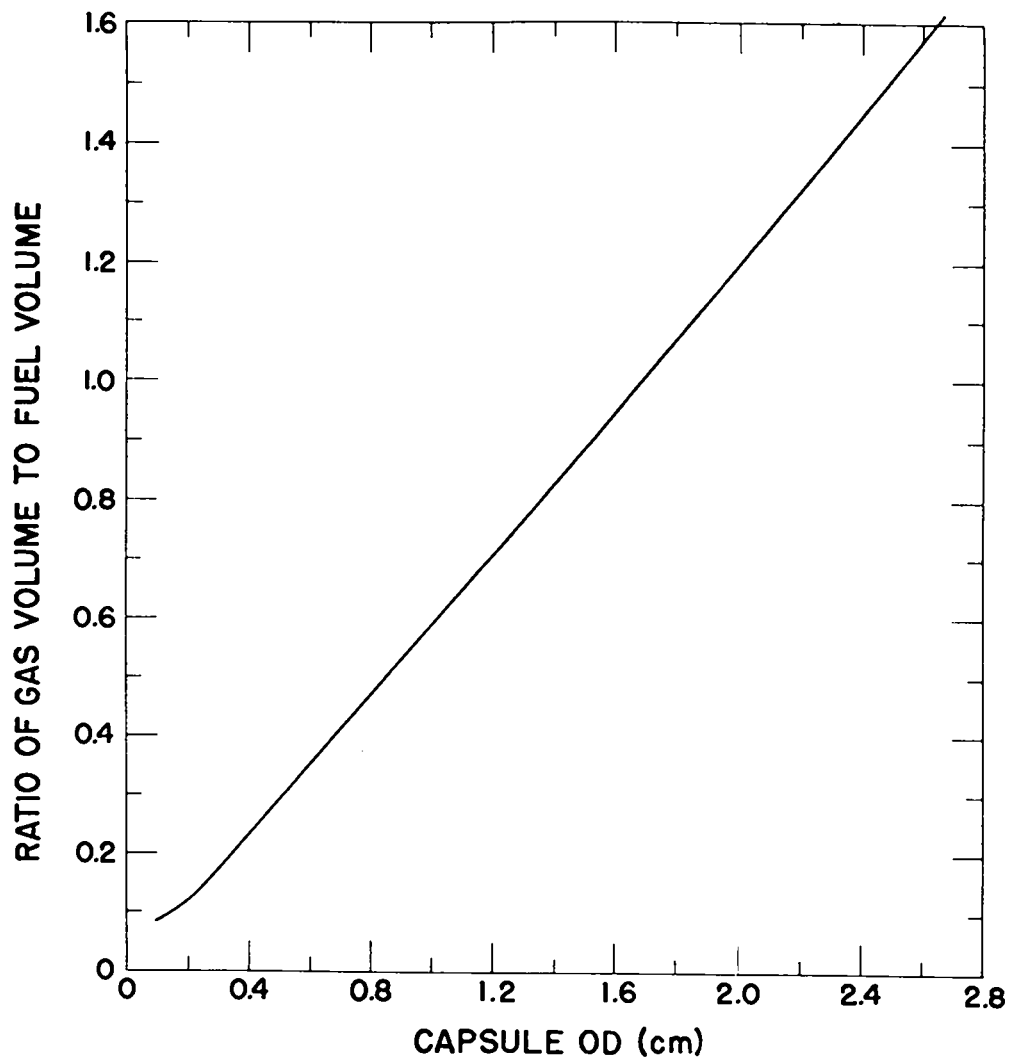
Fig. 8.  Plenum Volume Required for 1 gf/cc Burnup

# APPENDIX F

## Pu-Co-Ce ALLOY COMPOSITIONS

A full range of alloys of plutonium, cobalt, and cerium has been investigated. There is a eutectic valley, so that these are alloys containing from 0 to 15 g Pu/cc fuel which have melting points below 440°C. These are the fuels of current interest for power reactor application.

Compositions of a number of alloys in the eutectic valley have been calculated. The procedure used is as follows:

1.  Densities of pure plutonium, cerium, and cobalt at 500°C were calculated, assuming the metals were liquid at this temperature. The density of plutonium in the liquid state is[37]

    $$\text{liquid density} = 17.63 - 1.52 \cdot 10^{-3} \, T[°C].$$

    Therefore, if this were liquid at 500°C, the density would be 16.87 g/cc.

    The density of cobalt in the liquid state is apparently not well known. The density for the face-centered cubic structure (stable above 430°C) is 8.80 g/cc. An average thermal coefficient of expansion[38] of $14.5 \cdot 10^{-6}$/°C at 500°C is used for the solid phase. Thus, the solid density at 500°C is approximately 8.62 g/cc. With an average increase in the volume for metals on melting of $\approx 3\%$,[39] the liquid density would be approximately 8.36 g/cc.

    The cerium density is given in Ref. 40 for 806°C as 6.68 g/cc, and at 1000°C as 6.637 g/cc. Extrapolating back to 500°C gives a density of 6.75 g/cc.

2.  From the series of isotherms for the Pu-Co-Ce system, alloy compositions in the low-melting valley were selected. Those corresponding to particular values of plutonium concentrations (in g/cc) are given in Table F.1.

3.  The volume percent (v/o) of each constituent of the fuel over the entire range was calculated as follows:

$$\text{v/o Pu} = \frac{\text{g Pu/cc}}{16.87} \cdot 100$$

$$\frac{\text{v/o Ce}}{\text{v/o Co}} = \frac{\text{a/o Ce}}{\text{a/o Co}} \cdot \frac{\text{at. wt Co/cc liquid Co}}{\text{at. wt Ce/cc liquid Ce}} = \text{vol. ratio Ce/Co}$$

$$\text{v/o Ce} = (100 - \text{v/o Pu}) \frac{\text{vol. ratio Ce/Co}}{1 + \text{vol. ratio Ce/Co}}$$

4.  Densities were calculated based on

$$\rho(\text{alloy}) = (\text{vol. fraction Pu})(16.87[\text{g/cc}])$$
$$+ \text{vol. fraction Ce}(6.75[\text{g/cc}])$$
$$+ \text{vol. fraction Co}(8.36[\text{g/cc}])$$

5.  The weight percent (w/o) of each constituent at each composition was calculated from the relationship

$$\text{w/o of A} =$$

$$\frac{(\text{a/o of A})(\text{at.wt of A})}{(\text{at.fraction A})(\text{at.wt A}) + (\text{at.fraction B})(\text{at.wt B}) + (\text{at.fraction C})(\text{at.wt C})}$$

A measured density of 8.97 g/cc for a 3 g Pu/cc alloy corresponds favorably with the calculated 8.81 g/cc.

TABLE F.1

Calculated Densities of Liquid Pu-Co-Ce Alloys at 500°C for Perfect Solutions

| g Pu/cc | 0 | 1 | 2 | 3 | 4 | 5 | 5.7 | 7.6 | 8 | 9.5 | 11 | 13 | 15 |
|---|---|---|---|---|---|---|---|---|---|---|---|---|---|
| a/o plutonium | 0 | 7.1 | 13.7 | 20.1 | 26.2 | 32.0 | 35.8 | 46.0 | 48.2 | 56.2 | 64.5 | 75.6 | 86.5 |
| a/o cobalt | 25.0 | 25.0 | 25.0 | 25.0 | 24.8 | 24.8 | 24.7 | 23.5 | 22.95 | 21.4 | 18.1 | 13.9 | 9.38 |
| a/o cerium | 75.0 | 67.9 | 61.3 | 54.9 | 49.0 | 43.2 | 39.5 | 30.5 | 28.85 | 22.4 | 17.4 | 10.5 | 4.19 |
| v/o plutonium | 0 | 5.93 | 11.85 | 17.78 | 23.7 | 29.65 | 33.8 | 45.0 | 47.4 | 56.3 | 65.3 | 77.2 | 88.9 |
| v/o cobalt | 10.18 | 10.47 | 10.71 | 10.92 | 11.17 | 11.34 | 11.57 | 11.44 | 11.22 | 10.65 | 9.16 | 7.09 | 4.80 |
| v/o cerium | 89.82 | 83.6 | 77.5 | 71.3 | 65.1 | 59.0 | 54.6 | 43.6 | 41.4 | 33.0 | 25.6 | 15.72 | 6.3 |
| w/o plutonium | 0 | 13.37 | 24.55 | 34.4 | 42.9 | 50.5 | 55.0 | 66.0 | 68.1 | 75.3 | 81.5 | 88.7 | 94.8 |
| w/o cobalt | 12.3 | 11.63 | 11.05 | 10.55 | 10.03 | 9.65 | 9.35 | 8.32 | 7.98 | 7.08 | 5.63 | 4.03 | 2.53 |
| w/o cerium | 87.7 | 75.0 | 64.4 | 55.1 | 47.1 | 39.9 | 35.6 | 25.6 | 23.9 | 17.62 | 12.87 | 7.24 | 2.69 |
| Density (approx) | 6.92 | 7.52 | 8.13 | 8.81 | 9.32 | 9.93 | 10.36 | 11.50 | 11.74 | 12.62 | 13.50 | 14.66 | 15.83 |

APPENDIX G

INFLUENCE OF REPROCESSING ON DOUBLING TIME

The calculation of doubling time for much survey work neglects the influence of out-of-core inventory and of reprocessing losses. With certain simplifying assumptions, however, it is possible to obtain reasonable estimates of the significance of these factors.

The consumption rate of fissionable material in a breeder is

$$\text{Consumption rate[g fissioned/d]} = (p[\text{MW}])(a_1[\text{gf/MWd}])(F) \qquad (G.1)$$

where

$p$ is the reactor power

$a_1$ is the gf/MWd = 1/0.93

F is the plant capacity factor.

For an equilibrium plutonium isotopic composition, the consumption rate of plutonium is by fission only, and the fractional consumption rate of fissile and of total plutonium are the same.

The doubling time is normally defined in such a way that

$$(DT_0[\text{d}])(\text{Production rate} - \text{consumption rate})[\text{g/d}] = \text{Inventory[g]}.$$

Reprocessing losses may be includes symbolically by defining doubling time in such a way that

$$(DT[\text{d}])(\text{production rate} - \text{consumption loss rate[g/d]})$$

$$= (\text{Inventory} + \text{Losses[g]}), \qquad (G.2)$$

where losses[g] are reprocessing losses per doubling time.

93

Expression (G.2) is valid for any material or combination of material, so long as all terms apply to the material or materials in question. Considering fissile inventory, this may be written

$$DT_{fissile}[d] = \frac{\text{fissile inventory[g] + fissile losses[g]}}{(\text{fissile production rate - fissile consumption rate})[g/d]}$$

$$= \frac{\text{fissile inventory[g] + fissile losses[g]}}{(BR - 1)(\text{fissile consumption rate}[g/d])} \qquad (G.3)$$

For equilibrium plutonium and assuming that no other fissile material is present, this is the same as

$$DT_{Pu}[d] = \frac{\text{Pu inventory[g] + Pu losses[g]}}{(BR - 1)(\text{Pu consumption rate}[g/d])}$$

$$= \frac{\text{Pu inventory[g] + Pu losses[g]}}{(BR - 1)(P_{Pu}[MW])(a_1[gf/MWd])(F)} \qquad (G.4)$$

where

$P_{Pu}$ is the power produced from fission of plutonium (i.e., the reactor power less the $^{238}$U fast fission).

When translated to more common units, Eq. (G.4) with $a_1 = 1/0.93$ becomes

$$DT_{Pu}[yr] = \frac{(\text{Pu inventory[kg] + Pu losses[kg]})(10^3[g/kg])}{(BR - 1)(P_{Pu}[MW])(a_1[gf/MWd])(F)(365[d/yr])}$$

$$= \frac{(2.55[MW\text{-}yr/kg])(L_t[kg] + L_f[kg])}{(BR - 1)(P_{Pu}[MW])(F)} \qquad (G.5)$$

where

$L_t$ is the total plutonium inventory[kg]

$L_f$ is the total plutonium loss in one doubling time[kg].

We may now define an effective plutonium specific power by the relation

$$SP_P \equiv \frac{\text{plutonium power[MWt]}}{\text{plutonium inventory[kg]}} = \frac{P_{Pu}}{L_t}[\text{MWt/kg}].$$ (G.6)

This may be written

$$\frac{1}{SP_P} = \frac{L}{P_{Pu}} \left\{ 1 + \frac{(L_t - L)}{L} \quad [\text{kg/MWt}] \right\}$$ (G.7)

where

L is the in-core plutonium inventory

$(L_t - L)$ is the out-of-core plutonium inventory.

The ratio of out-of-core to in-core inventory is approximately equal to the ratio of out-of-core to in-core time. The actual average out-of-core inventory may be somewhat less because of burnup. The in-core time is related to the fuel burnup by the relation

$$t_{\text{in-core}}[\text{d}] = \frac{(0.93 \cdot 10^3 [\text{MWd/kgf}])(BU[\text{gf/cc}])}{(SP_c[\text{MW/kg}])(\rho_c[\text{g/cc}])(F)}$$ (G.8)

where

$SP_c$ is the core specific power[MW/kg]

$\rho_c$ is the plutonium density[g/cc]

BU is the core burnup[gf/cc].

The time out-of-core is fixed by reprocessing requirements and will be written simply $t_{\text{out}}$. Thus,

$$\frac{(L_t - L)}{L} \simeq \frac{t_{\text{out}}}{t_{\text{in-core}}}$$

$$= \frac{(t_{\text{out}}[\text{d}])(SP_c[\text{MW/kg}])(F)(\rho_c[\text{g/cc}])}{(0.93 \cdot 10^3 [\text{MWd/kgf}])(BU[\text{gf/cc}])}$$ (G.9)

Combining this with Eq. (G.7),

$$\frac{1}{SP_P} = \frac{L}{P_{Pu}} + \frac{(t_{out}[d])(\rho_c[g/cc])(F)}{(0.93 \cdot 10^3[MWd/kgf])(BU[gf/cc])} \cdot \left\{ (SP_c) \frac{L}{P_{Pu}} \right\} \quad . \qquad (G.10)$$

Quantitatively, the term $(P_{Pu}/L)$ is approximately the same as the core specific power. For the liquid fuel case, a beginning-of-life core specific power with a clean blanket is an in-core plutonium specific power. The buildup of blanket power and the contribution of core non-plutonium power limit the range of validity of this assumption. Since the ratio of $(SP_c)$ to $(P_{Pu}/L)$ appears in a correction term, errors will have only a second order effect on doubling time. Thus, this ratio will be taken to have a value of unity. Thus, using Eq. (G.5),

$$DT[yr] = \frac{2.55(1 + L_f/L_t)}{(F)(BR - 1)} \left\{ \frac{L}{P_{Pu}} + \frac{t_{out} \cdot \rho_c \cdot F}{(0.93 \cdot 10^3) \cdot BU} \right\} \qquad (G.11)$$

It remains to relate $L_f$, the loss per doubling time, to more common factors. The total plutonium loss rate can be written:

$$L_f[kg] = R_0 \cdot \text{plutonium mass reprocessed per doubling time}$$

$$= R_0 \cdot K \cdot L[kg] \qquad (G.12)$$

where

    $R_0$ is the fractional loss during reprocessing

    K is the number of core masses reprocessed per doubling time

    L is the core plutonium loading.

Again, a correction term could be used to account for the difference among L, the quantity of clean fuel subject to fabrication loss, and the quantity of irradiated fuel to be reprocessed. The net effect of such a correction is small. But, from the definition of doubling time,

we may write:

$$K(\text{core cycles}) \cdot (\text{net kg gained/core cycle}) = L_t.$$

The total burnup per core cycle[kg] is

$$\frac{BU[gf/cc]}{\rho_f[g/cc]} \cdot (L[kg])$$

so that the gain per cycle[kg] is

$$(BR - 1) \frac{BU[gf/cc]}{\rho_c[g/cc]} L[kg].$$

Thus,

$$K = \frac{L[kg]}{(BR - 1) \dfrac{BU[gf/cc]}{\rho_c[g/cc]} L[kg]} = \frac{(\rho_c[g/cc])(L_t[kg])}{(BU[gf/cc])(BR - 1)(L[kg])} \cdot \qquad (G.13)$$

Combining this with Eq. (G.12) yields

$$\frac{L_f}{L_t} = \frac{R_0 \, \rho_c}{BU(BR - 1)} \cdot \qquad (G.14)$$

Equation (G.11) then becomes

$$DT = \frac{2.55[MWd/kg]\left[1 + \dfrac{R_0 \, \rho_c}{BU(BR - 1)}\right]}{(BR - 1)(F)}\left\{\frac{L[kg]}{P_{Pu}[MW]} + \left(\frac{t_{out}[d] \cdot \rho_c[g/cc] \cdot F}{0.93 \cdot 10^3[MWd/kgf] \; BU[gf/cc]}\right)\right\}$$

$$(G.14)$$

The influence of these factors on the doubling time of the two
systems considered is shown in Table G.1. A low-gain breeder is also
included for illustration.

97

TABLE G.1

Influence of Reprocessing Factors on Doubling Time

| Input Factors[a] | Units | Symbol | Solid Fuel | Liquid Fuel | Low-Gain Breeder |
|---|---|---|---|---|---|
| Breeding Gain | --- | $(BR - 1)$ | 0.49 | 0.37 | 0.15 |
| Load factor | --- | $F$ | 0.8 | 0.8 | 0.8 |
| Fractional loss during reprocessing | --- | $R_0$ | 0.02 | 0.02 | 0.02 |
| Core plutonium density | [g/cc] | $\rho_c$ | 2.4 | 3.7 | 2.0 |
| Burnup | [gf/cc] | $BU$ | 1.0 | 1.0 | 1.0 |
| In-core plutonium inventory | [kg] | $L$ | 3700 | 2700 | 3000 |
| Plutonium power | [MWt] | $P_{Pu}$ | 1800 | 1900 | 1800 |
| Out-of-core time | [d] | $t_{out}$ | 250 | 100 | 250 |

Inferred Doubling Times [yr]

| | | | | | |
|---|---|---|---|---|---|
| No losses or out-of-core inventory | | | 13.4 | 12.2 | 35.4 |
| No losses but with out-of-core inventory | | | 16.7 | 15.0 | 44.6 |
| With losses, but no out-of-core inventory | | | 14.7 | 14.7 | 44.9 |
| With losses and out-of-core inventory | | | 18.4 | 18.0 | 56.5 |

---

[a] The figures given are illustrative. A fixed nominal density is used. $t_{out}$ is assumed to be fixed by required cooling times.

APPENDIX H

ESTIMATED AVERAGE COMPOSITIONS AT SEVERAL TIMES IN A CYCLE

It is frequently convenient to estimate compositions at several stages of burnup prior to performing detailed burnup calculations. This allows the selection of a suitable range of parameters for detailed study.

In most studies to date, the core region has been limiting. Therefore, most performance specifications are expressed in terms of core parameters. It is, in general, straightforward to estimate the core composition at various steps in life in terms of these specifications. It is appropriate to use blanket compositions which are consistent with the core parameters to avoid the introduction of an unintentional bias. Average blanket compositions can be obtained from material balance considerations.

Core compositions are normally specified in terms of the following parameters:

$\rho_0^x$ = initial concentration [g/cc] of material x in the core

$BU^x$ = burnup [g/cc] of material x

$ICR$ = internal conversion ratio

$P_c^{28}$ = core fractional power from fertile material (including $^{240}Pu$)

If the following parameters are known, the average blanket composition corresponding to any specified core burnup can be determined:

$\rho_0^x$ = initial concentration [g/cc] of material x in the core

$P_B$ = blanket power fraction

$P_B^{28}$ = blanket fractional power from fertile material

$BR$ = overall average breeding ratio

$V_r$ = core-to-blanket volume ratio

These factors can generally be obtained or reliably estimated.

The core compositions are estimated using the following generali-
zations and approximations:

1.  Total heavy atom content is the initial content less burnup

$$(\rho^{HA} = \rho^{HA}_0 - BU).$$

2.  Fissile content is the initial content of the fissile material,
    less its burnup, plus internal production of that material.  Fissile
    burnup is total burnup times the core fractional power from fissile
    material $\{BU(1 - P^{28}_c)\}$; internal production is internal conversion
    ratio times fissile burnup $\{BU(1 - P^{28}_c)ICR\}$.

The calculation of blanket compositions is illustrated by the solid-
fuel system and a liquid-fuel system, each with an oxide blanket.  The
core parameters used are:*

|  | Solid Fuel | Liquid Fuel |
|---|---|---|
| $\rho^{HA}_0$ [g/cc core] = | 3.55 | 1.4 |
| $\rho^{Pu}_0$ [g/cc core] = | 0.790 | 1.4 |
| BU[gf/cc core] = | 0.355 | 0.35 |
| ICR = | 0.6 | 0.1 |
| $P^{28}_0$ = | 0.26 | 0.1 |

The blanket parameters are:

|  | Solid Fuel | Liquid Fuel |
|---|---|---|
| $\rho^{HA}_0$ [g/cc blanket] = | 4.77 | 4.77 |
| $\rho^{fissile}_0$ [g/cc blanket] = | 0.014 | 0.014 |
| $P_B$ = | 0.2 | 0.28 |
| $P^{28}_B$ = | 0.12 | 0.4 |
| BR = | 1.4 | 1.4 |
| $V_r$ = | 0.70 | 0.165 |

---

*Note that these are expressed per unit core or blanket volume, rather
than as concentrations in the fuel.  Thus, these differ from values
previously used by a fuel volume fraction.

From these, we may infer the following:

| Step | Core | Units | Carbide (one cycle) | Liquid Plutonium (one cycle) |
|------|------|-------|---------------------|------------------------------|
| #1 | Gross plutonium burnup $BU(1 - P_c^{28})$ | [gf/cc core] | 0.263 | 0.35 |
| 2 | Core plutonium production ICR · #1 | [g/cc core] | 0.158 | 0.035 |
| 3 | Net core plutonium burnup #2 − #1 | [gf/cc core] | 0.105 | 0.315 |
| | **Blanket** | | | |
| 4 | Equivalent[a] total burnup $\dfrac{BU}{(1 - P_B)}$ | [gf/cc core] | 0.444 | 0.486 |
| 5 | Blanket burnup equivalent #4 · $P_B$ | [gf/cc core] | 0.0888 | 0.1363 |
| 6 | Blanket burnup #5 · $V_r$ | [gf/cc blanket] | 0.0633(1.3%) | 0.0225(0.47%) |
| 7 | Gross blanket fissile burnup, equivalent #5$(1 - P_B^{28})$ | [g Pu f/cc core] | 0.0781 | 0.0817 |
| 8 | Gross total fissile burnup, equivalent #7 + #1 | [g Pu f/cc core] | 0.341 | 0.397 |
| 9 | Total plutonium production, equivalent #8 · BR | [gf/cc core] | 0.477 | 0.556 |
| 10 | Blanket plutonium production, equivalent #9 − #2 | [g/cc core] | 0.319 | 0.521 |
| 11 | Net blanket fissile, equivalent #10 − #7 | [g/cc core] | 0.241 | 0.439 |
| 12 | Net blanket fissile #11 · $V_r$ | [g/cc blanket] | 0.169 | 0.072 |
| 13 | Final blanket fissile $\rho_0$ + #12 | [g/cc blanket] | 0.183(3.84%) | 0.086(1.81%) |
| 14 | Final blanket heavy atom density $\rho_0$ − #6 | [g/cc blanket] | 4.71 | 4.75 |

[a] Equivalent factors are expressed as if contained with in-core volume.

# REFERENCES

1. R. P. Hammond et al., "Mobile Fuel Plutonium Breeders. A Study of Economic Potential," LA-2644, Los Alamos Scientific Laboratory (1961).

2. W. H. Hannum and L. D. Kirkbride, "The Molten Plutonium Burnup Experiment," LA-3384-MS, Los Alamos Scientific Laboratory (1966).

3. W. H. Hannum et al., "An Application of Molten Plutonium to Fast Breeders," in "Proceedings of the Conference on Breeding, Economics, and Safety in Large Fast Power Reactors," ANL-6792, Argonne National Laboratory (1963).

4. "Liquid Metal Fast Breeder Reactor Design Study," WCAP-3251-1, Westinghouse Electric Corporation (1964).

5. C. A. Pursel and L. E. Link, "1000-MWe Sodium-Cooled Fast Breeder Reactor Studies," in Proceedings of the British Nuclear Energy Society Fast Breeder Conference, May 1966 (to be published).

6. "Large Fast Reactor Design Study," ACNP-64503, Allis-Chalmers (1964).

7. "Liquid Metal Fast Breeder Reactor Design Study," CEND-200, Combustion Engineering (1964).

8. "Liquid Metal Fast Breeder Reactor Design Study," GEAP-4418, General Electric (1964).

9. "Feasibility Study of a 1000-MWe Sodium-Cooled Fast Reactor," NAA-SR-11378, Atomics International (1965).

10. D. Smidt et al., "Referenzstudie fur den 1000 MWe Natriumgekuhlten Schnellen Brutreaktor (Na 1)," KFK-299, Kernforschungszentrum, Karlsruhe (1964).

11. "An Evaluation of Four Design Studies of a 1000 MWe Ceramic Fueled Fast Breeder Reactor," COO-279, Chicago Operations Office, USAEC (1964).

12. "An Evaluation of the Atomics International 1000 MWe Fast Breeder Reactor," COO-285, Chicago Operations Office USAEC (1966).

13. B. Carlson et al., "DTF Users Manual," UNC Phys & Math-3321, United Nuclear Corporation (1963).

14. W. J. Worlton and B. Carlson, "The DDF Code," an unpublished Los Alamos Scientific Laboratory code.

15. G. E. Hansen and W. H. Roach, "Six and Sixteen Group Cross Sections for Fast and Intermediate Critical Assemblies," LAMS-2543, Los Alamos Scientific Laboratory (1961).

16. "Guide to Nuclear Power Cost Evaluation," TID-7025, Kaiser Engineers, Division of Henry J. Kaiser Company (1962).

17. L. D. Kirkbride, "Molten Plutonium Alloys as Fast Reactor Fuels," in "Proceedings of the Conference on Safety, Fuels, and Core Design in Large Fast Power Reactors," ANL-7120, Argonne National Laboratory (1966).

18. M. J. Whitman et al., "Fast Breeder Development in the United States," in Proceedings of the British Nuclear Energy Society Fast Breeder Conference, May 1966 (to be published).

19. A. G. Frame et al., "Design of the PFR," in Proceedings of the British Nuclear Energy Society Fast Breeder Conference, May 1966 (to be published).

20. M. Levinson et al., "Comparative Cost Study of the Processing of Oxide, Carbide, and Metal Fast-Breeder-Reactor Fuel by Aqueous, Volatility, and Pyrochemical Methods," ANL-7137, Argonne National Laboratory (1966).

21. "LAMPRE Final Report," Los Alamos Scientific Laboratory (in preparation).

22. H. I. Bowers, "The HTHX-2 Code," an unpublished Los Alamos Scientific Laboratory code.

23. W. H. Hannum and B. M. Carmichael, "DPC -- A Two-Dimensional Data Preparation Code," LA-3427-MS, Los Alamos Scientific Laboratory (1966).

24. J. A. Leary et al., "Pyrometallurgical Purification of Plutonium Reactor Fuels," Proc. U.N. Intern. Conf. Peaceful Uses At. Energy, 2nd, Geneva, 1958, v. 17, p. 376 (Pub. 1958 and 1959).

25. L. J. Mullins et al., "Plutonium Electrorefining," LA-2666, Los Alamos Scientific Laboratory (1962).

26. L. J. Mullins et al., "Large Scale Preparation of High Purity Plutonium Metal by Electrorefining," LAMS-2441, Los Alamos Scientific Laboratory (1960).

27. J. J. Prabulos, Jr., "DTF-BURN, A Multigroup Transport Theory Burnup Program Written in FORTRAN-IV," LA-3671, Los Alamos Scientific Laboratory (1967).

28. "Los Alamos Group-Averaged Cross Sections," L. D. Connolly, ed., LAMS-2941, Los Alamos Scientific Laboratory (1963).

29. W. Murgatroyd, "Thermal Convection in a Long Cell Containing a Heat Generating Fluid," AERE-ED/R-1559, Atomic Energy Research Establishment, Harwell, England (1954).

30. W. H. Corcoran et al., "Temperature Gradients in Turbulent Gas Streams," Ind. Eng. Chem. 44, 410 (1952).

31. L. Onsager and W. W. Watson, "Turbulence in Convection in Gases Between Concentric Vertical Cylinders," Phys. Rev. 56, 474 (1939).

32. J. Woodrow, "Free Convection in Heat Generating Fluid (Laminar Flow)," AERE-E/R-1267, Atomic Energy Research Establishment, Harwell, England (1953).

33. O. E. Dwyer, "Eddy Transport in Liquid-Metal Heat Transfer," BNL-6046, Brookhaven National Laboratory (1962).

34. C. A. Anderson, Jr., "Fission Product Yields from Fast ($\simeq 1$ MeV) Neutron Fission of Pu-239," LA-3383, Los Alamos Scientific Laboratory (1965).

35. S. H. Maron and C. F. Prutton, Principles of Physical Chemistry, 3rd edition, Macmillan, New York, 1958.

36. J. O. Hirschfelder et al., Molecular Theory of Gases and Liquids, Wiley, New York, 1954.

37. C. Z. Serpan, Jr., and L. J. Wittenberg, "The Density of Liquid Plutonium Metal," Trans. Met. Soc. AIME 221, 1017 (1961).

38. C. A. Hampel, Rare Metals Handbook, Reinhold, New York, 1961.

39. L. S. Darken and R. W. Gurry, Physical Chemistry of Metals, McGraw-Hill, New York, 1953.

40. Data provided by Mound Laboratory, private communication from L. J. Wittenberg.

LIST OF SYMBOLS

| | | | | |
|---|---|---|---|---|
| A | Absorption rate | Pr | Prandtl number |
| $A_t$ | Capsule wall coefficient of thermal expansion | $P_B$ | Blanket power fraction |
| $a_1$ | Grams fissioned/MWd = 1/0.93 | $p_c^{28}$ | Fraction of core power generated in fertile material |
| BF(R) | Radial breeding factor; a one-dimensional estimate of contributions of core and radial (but not axial) blanket to the breeding ratio | p | Internal pressure of gas in capsule |
| | | P/D | Pitch-to-diameter ratio in fuel lattice |
| | | $\Delta p$ | Core coolant pressure drop |
| BR | Breeding ratio | $Q'$ | Total core power per unit fuel height |
| BU | Burnup [gf/cc] | $R_0$ | Fractional loss during reprocessing |
| $c^i$ | Capture rate in region i | R | Gas constant |
| $C_p$ | Specific heat of the coolant | Re | Reynolds number |
| D | Capsule outside diameter | S | Stress |
| $D_{ep}$ | Equivalent diameter for pressure drop calculation | $S_i$ | Neutron source in region i |
| | | $SP_c$ | Reactor power/in-core inventory |
| $D_{eH}$ | Equivalent diameter for heat transfer | SP | Reactor power/total cycle inventory |
| $DT$ | Reactor cycle doubling time | $SP_f$ | Reactor power/in-core fissile inventory |
| $DT_0$ | Core inventory doubling time | T | Temperature |
| E | Plutonium fissile fraction = $L_f/L$ | $T_{in}$ | Core coolant mixed mean inlet temperature |
| E | Elastic modulus | t | Capsule wall thickness |
| f | Friction factor | $t_{in-core}$ | Average in-core residence time |
| F | Capacity factor [full power days/day] | $t_{out}$ | Average out-of-core time required for fuel during the fuel cycle |
| g | Gravitational constant = 980 cm/sec$^2$ | | |
| H | Film heat transfer coefficient | $\Delta T_F$ | Coolant film temperature drop |
| h | Core fuel length | $\Delta T_M$ | Mixed mean core coolant temperature rise |
| ICR | Internal conversion ratio | $\Delta T_W$ | Temperature drop across capsule wall |
| K | Number of reprocessing cycles per doubling time | $V_F$ | Fuel volume |
| | | $V_m$ | Molar volume of gas in capsule |
| $k_N$ | Coolant thermal conductivity | $V_r$ | Core-to-blanket volume ratio |
| $k_W$ | Capsule wall thermal conductivity | v | Coolant velocity |
| $L$ | Neutron leakage term | W | Coolant mass flow rate |
| $L_f$ | Total nonconstructive loss of fissile material in one doubling time | z | Distance along core fuel, from 0 to h. |
| L | In-core plutonium inventory | $\alpha_f$ | Capture-to-fission ratio of the core plutonium |
| $L_f$ | In-core fissile inventory | $\alpha$ | Gas-to-fuel volume ratio |
| $L_t$ | In-core plus out-of-core plutonium inventory | $\alpha_i$ | Source-to-absorption ratio in region i |
| (M/A) | Maximum-to-average core power ratio | $\phi$ | Neutron flux |
| $(M/A)_R$ | Radial maximum-to-average core power ratio | $\bar{\psi}$ | Ratio of heat transfer eddy diffusivity to momentum transfer eddy diffusivity |
| N | Number of fuel capsules | $\upsilon$ | Poisson's ratio |
| $N_0$ | Avogardro's number = 6.02 · 10$^{23}$ | $\nu$ | Neutrons/fission |
| $N_{min}^a$ | Minimum number of capsules consistent with constraint a | $\rho_N$ | Density of coolant |
| Nu | Nusselt number | $\rho_f$ | Density of fissile plutonium in the core fuel |
| p | Reactor power | | |
| $P_{Pu}$ | Reactor power from plutonium | $\rho_c$ | Density of plutonium in the core fuel |
| $P_c$ | Core power fraction | $\Sigma_x^i$ | Cross section of material i for process x |
| P | Capsule center-to-center spacing | | |